A MODEL FOR LIQUID FLOW DISTRIBUTION IN TRICKLE-BED REACTORS

A Thesis Submitted
in Partial Fulfilment of the Requirements
for the Degree of
MASTER OF TECHNOLOGY

by

A. SUBRAHMANYA SASTRY

to the

Department of Chemical Engineering
Indian Institute of Technology, Kanpur
March, 1996

CERTIFICATE

This is to certify that the present research work entitled **A Model for Liquid Flow Distribution in Trickle-bed Reactors** *has been carried out by* **A. Subrahmanya Sastry** *under my supervision and it has not been submitted elsewhere for a degree.*

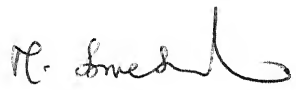

Dr. M. S. Rao
Professor
Dept. of Chemical Engineering
Indian Institute of Technology
Kanpur

March 1996

ABSTRACT

Trickle-bed reactors are three-phase reactors in which gas and liquid flow down cocurrently through a fixed bed of catalyst particles. A model for liquid flow distribution in trickle-bed reactors is presented assuming complete wetting of the particles. The model uses a computer generated, three-dimensional sphere pack as the porous medium and liquid flow is simulated through particle-particle contacts. Exit liquid flow distributions from the bed are depicted as three-dimensional histograms. Effect of inlet distributor configuration, liquid flow rate and diameter of the particle are studied. These results are compared with recently reported experimental work. The phenomena of channelling and bed scale partial wetting observed in nonprewetted beds is satisfactorily represented through simulations. Bed scale complete wetting which was observed with all the inlet configurations of prewetted bed is also satisfactorily represented.

ACKNOWLEDGEMENTS

I express my deep gratitude, respectful regards and sincere thanks to my teacher, Dr. M. S. Rao, for his constant encouragement and discerning guidence throughout the course of this work.

I take this opportunity to express my sincere thanks to Dr. D. P. Rao and Dr. Ashutosh Sharma for providing valuable suggestions which proved very fruitful towards the end.

I have no words to express my feelings of gratitude towards Mr. P. V. Ravindra. My sincere thanks to him for his painstaking efforts in the odd hours. My special thanks are due to pavitra for his stimulating discussions and timely help.

I greatfully acknowledge the financial support provided by Engineers India Ltd. in carrying out this work.

Chakri, Bullu, Prasad, poorna and kali might not have recognized what their presence had in my stay. I am thankful to vidya, Gupta, wkm, band, Ravi, Mukthi, Murthy, Vasant, Anil and my other friends. It's been pleasure sharing moments with them.

Finally, to my parents and siblings goes my eternal gratitude for their constant love and support.

- Sastry

TABLE OF CONTENTS

LIST OF FIGURES

LIST OF TABLES

NOTATION

d_p	particle diameter, cm
D_r	coefficient of radial spread of liquid, cm
f_w	mean local flow density, cm/s
g	acceleration due to gravity, cm/s^2
L	superficial mass flow rate of liquid, $kg/m^2.s$
L_{min}	minimum mass flow rate of liquid to attain complete wetting, kg/s
m	minimum flow rate required to wet unit length of surface, kg/m.s
q_c	minimum volumetric flow rate of liquid required for complete weting of a spherical particle, cm^3/s
q_t	total volumetric flow rate of liquid to a particle, cm^3/s
S	Length of the grain boundary, cm
w	Dimension of the box in xy-plane, cm
x	bed coordinte in x direction, cm
y	bed coordinte in y direction, cm
z	bed coordinte in z direction, cm

Greek letters

μ	viscosity of liquid, poise
ϕ	Potential field
ρ	density of the liquid, g/cm^3
σ	surface tension of liquid, dynes/cm
θ	angle measured from the vertical axis of the sphere

CHAPTER 1

INTRODUCTION

Multiphase reactors are those reactors in which two or more phases are necessary to carry out the reaction. The majority of multiphase reactors involve gas and liquid phases which contact a solid phase. These can be broadly classified into two categories: one, where the solids form a fixed bed,and the other, where the solids are suspended in the liquid. Fixed bed reactors with cocurrent down flow or up flow of fluid phases come under the first category. The latter category includes stirred slurry reactors, bubbling slurry reactors and fluidized slurry reactors. A trickle-bed reactor can be defined as a fixed bed of catalyst particles, contacted by gas-liquid, two-phase flow. The flow may be co-current(downflow or upflow) or countercurrent. However, because of its relatively lower pressure drop and absence of flooding, cocurrent downflow is by far the most common mode of operation in industrial practice.

Trickle-bed reactors are primarily used in the petroleum industry in processes such as hydrodesulfurization, denitrogenation, demetallation of various petroleum fractions, and liquid phase catalytic hydrocracking. Other commercial applications of trickle-bed reactors can be found in the petrochemical industry, involving hydrogenation and oxidation of organic compounds, where the gaseous reactant is sparingly soluble in the liquid phase. These applications include synthesis of butynediol from formaldehyde and acetylene, hydrogenation of aniline to cyclohexylaniline, hydrogenation of cyclohexene to cyclohexane etc.

In waste water treatment plants trickle bed reactors are used as trickling filters to remove organic matter from waste water streams by aerial bacterial action. In these units biological growth is allowed ot attach itself to a bed of stones or other supports over which the waste water is allowed to trickle in contact with air. These reactors can also be used for the removal of pollutants from a gas stream and also to dissolve the gaseous reactants in liquid phase as in polymerization of ethylene or hydrogenation of oils. They are also being considered for biological systems where enzymes, immobilized on the pores and surface of the packings are employed to catalyze reactions between the gas and liquid phases.

Trickle-bed reactors are physically similar to the packed bed absorption columns except for these differences: 1) Trickle-beds are operated at very low liquid and gas velocities, while packed bed absorbers are operated at fairly high gas and liquid velocities. 2) In trickle-beds, packing is a porous active catalyst which is usually in the form of spherical or cylindrical pellets, while in packed bed absorbers, packing is an inert material which improves gas liquid contacting.

The advantages of trickle-bed reactors, as compared to other types of three-phase reactors, are: 1) high conversion in a single pass, 2) elimination of the need for catalyst separation, 3) no loss of catalyst , 4) low pressure drop and no flooding, 5) lower maintenance costs due to the absence of moving parts, and 6) high catalyst loading per unit volume of the liquid. Major disadvantages are poor heat transfer characteristics, lower catalyst effectiveness, and sensitivity of reaction rates to flow regimes.

The superficial liquid velocities encountered in trickle-beds range from 0.01 to 0.3 cm/sec in pilot plant reactors and from 0.1 to 2 cm/s in commercial reactors. The superficial gas velocity ranges from 2 to 45 cm/s in pilot plant reactors and from 15 to 300 cm/s in commercial reactors. These are indicative ranges of flow rates and not definitive. Depending on the gas and liquid flow rates and the physical properties of the

liquid, wetting properties of the solid, and nature of the porous structure in the packed bed, various flow regimes may exist in a trickle-bed. A knowledge of this is essential in understanding the hydrodynamics and mass transfer characteristics. Sato et al. (1973) observed various flow regimes in co-current downflow packed bed reactor using glass spheres of 2.59 - 16.5 mm diameter. They classified these flow regimes into three distinct flow patterns.

1) At a low liquid rate, the flow pattern is trickling, where the liquid trickles over the packing essentially in a laminar flow. Here the flow in one phase is not significantly affected by flow in the other phase and is known as low-interaction regime. 2) At higher gas and/or liquid rates the interaction between the gas and liquid phases is rather high and is known as high interaction regime or pulsing flow. 3) At very high liquid flow rates greater than 3 cm/s and low gas rates, the liquid becomes continuous phase and the gas flows as a dispersed phase in the form of bubbles. This is referred to as the dispersed bubble flow regime.

On the bed scale, four major flow patterns or flow regimes can be identified: trickling flow, pulsing flow, spray flow and bubble flow. 1) The *trickling flow* regime appears at relatively low gas and liquid input flow rates. In this regime, the liquid flows down the column from particle to particle on the surface of the packings while the gas phase travels in the interstitial void space of the flow channels. 2) *Pulsing flow* occurs at relatively high gas and liquid input flow rates. It refers to the formation of slugs that have a higher liquid content than the remainder of bed. 3) *Spray flow* regime occurs when the gas flow rate is high while the liquid flow rate is kept at a low value. The liquid is entrained down the bed by the continuous gas phase in the form of liquid droplets. 4) When the bed is filled with liquid, the gas phase pulses down the bed in the form of elongated bubbles. If the gas flow rate is increased at this point then the bubbles become highly irregular in shape. This is known as *dispersed bubble flow* regime.

In spite of many advantages, the potential of trickle-bed reactor has never been fully exploited due to poor understanding of the gas and liquid flow phenomena. The scale-up of trickle-bed reactors in petroleum processing is a proprietary industrial art for specific feed stocks and processes (Dudukovic and Mills, 1986).

Current practice in trickle-bed reactor design relies on empirical correlations for the different reactor parameters such as liquid holdup, the volume of liquid per unit volume of bed, wetting efficiency and the gas and liquid flow rates. Scaleup studies in trickle-bed reactors are essential due to three reasons. First, the development of truly comprehensive correlations has been low due to a large number of variables, reaction kinetics, bed porosity, size and shape of catalyst particles, interfacial tension, wettability, gas and liquid flow rates and viscosities, which have a considerable effect on the reactor operation. Secondly, even if we can find a correlation that is based on the same packings and similar fluids as the commercial reactor and covers the range of operating conditions anticipated, another major problem exists. Depending on the manner in which the packings are packed and the gas and liquid distributors are configured, the flow pattern in a commercial reactor may differ markedly from that of the laboratory-scale reactor from which the correlation was obtained. As a result, the degree of uncertainty about the acceptability and accuracy of a correlation may not be acceptable for reactor design. Thirdly, many basic aspects of trickle-beds are not fully understood, making design from fundamentals rather difficult.

Despite the incomplete understanding of reactor behavior, several models have been proposed in the literature to predict the performance of trickle-bed reactors. In the earlier studies, mass transport effects¿were neglected, and gas and liquid phases were treated as a single homogeneous phase (pseudo-homogeneous models). The catalyst particles are assumed to be partially wet and the reaction was assumed to occur only in the wetted zones of the catalytic bed, in order to have a simple relationship between the apparent

rate and the extent of contact between liquid and solid. The apparent reaction rate was assumed to be proportional to the liquid holdup (Henry and Gilbert, 1973), and to the fractional coverage of the catalyst surface with the flowing liquid, known as wetting efficiency (Mears, 1974). These pseudo-homogeneous models are able to predict the behavior of trickle-bed reactors for liquid limiting reactions such as hydrodesulfurization of heavy distillates (Paraskos et al., 1975), hydrodenitrogenation of hydrotreated oils (van Klinken and van Dongen, 1980), and decomposition of hydrogen peroxide over activated carbon (Koros, 1976) etc.

However, when the limiting reactant is present in the gas phase, a minimum in the reaction rate was observed for hydrogenation of α-methylstyrene (Herskowitz et al., 1979) and oxidation of sulfur dioxide (Mata and Smith, 1981). The pseudo-homogeneous models fail to predict the observed reaction rate trends. Heterogeneous models accounting for external mass transfer resistance have been proposed to explain the minimum in the reaction rate. In these models, both the wetted and unwetted zones of the catalyst particles were assumed to contribute to the reaction rate. The gaseous reactant must overcome both the gas-liquid, and liquid-solid mass transfer resistances of the flowing liquid film to reach the wetted catalyst pellet, whereas on the nonwetted surface, the gaseous reactant is in direct contact with the liquid in the pores. Some investigators assumed that the nonwetted surface of the catalyst is covered with a stagnant liquid film and offers a significant resistance to the transport of gaseous reactant (Mills and Dudukovic, 1984), whereas others assumed that the dry surface is devoid of liquid film (Herskowitz et al., 1979; Capra et al., 1982; among others).

Considerable work has been done to find the wetting efficiency since it is an important parameter in interpreting the reaction rate data in both the homogeneous and heterogeneous models. Techniques such as stimulus response (tracer), dissolution, and chemical methods have been employed to determine the wetting efficiency. However, there is no di-

rect experimental evidence of partial wetting of catalyst particles in a trickle-bed reactor. On the other hand, a theoretical study (Reddy et al., 1990) based on the characteristics of largest stable, static pendular rings, suggests that there may not be dry patches over particles in trickle-beds packed with particles less than about 4 mm diameter.

Modeling of various transport processes and reaction rates requires the knowledge of liquid flow texture, i.e., the particle-scale and bed-scale distribution of liquid and the associated flow field. The presence of multiple hydrodynamic states (Kan and Greenfield, 1978; Christensen et al., 1986), flickering hot spots (Germain et al., 1974; Jaffe, 1976), slow transients at low liquid flow rates (Haure et al., 1992) etc. have also brought to focus the need for understanding the liquid flow texture in trickle-beds.

In the trickling regime, the liquid flow texture has been visualized to comprise of films, rivulets, pendular rings and liquid bridges on particle-scale, and liquid pockets and filaments on bed-scale (Lutran et al., 1991). The extent to which these flow features are present dictates the pressure drop, liquid holdup, gas-liquid and liquid-solid interfacial areas, and reaction rates. There are a few reports on the liquid flow texture in packed beds, but the observations were confined to the proximity of the walls as the interior of the bed remained inaccessible due to the lack of suitable experimental techniques.

Maldistribution in a trickle-bed reactor can be due to any one of following reasons:

1) Poorly designed liquid distributor. 2) The way catalyst particles are packed (Particularly susceptible to this this sort of maldistribution are a bed of cylindrical extrudates). 3) Another form of maldistribution can be in reactors with highly exothermic reactions. As the liquid film flows down in the column from particle to particle, vaporization takes place and particles near the bottom are without a liquid film to carry away the heat generated which leads can lead to hot spot formation.

On this important factor of trickle-bed operation, number of theories have been de-

veloped to predict the liquid flow distribution in trickle-bed reactors. Models based on percolation concepts (Crine et al., 1980; Melli and Scriven, 1991; among others), and models that utilize computer generated sphere packs and spread of liquid from sphere to sphere (Zimmerman and Ng, 1986; Funk et al., 1990) have been few of them. However, the premises used in modeling the liquid flow distribution were not based on experimental findings. For example, none of these models takes into account whether the bed is prewetted or not, whereas prewetting of the bed has been shown to significantly influence the liquid flow texture in the bed (Lutran et al., 1991).

The objectives of the present work are :

(i) to develop a model for liquid flow distribution in a trickle-bed reactor considering the effect of start up procedure i.e prewetted and nonprewetted bed.

(ii) to study the effects of particle diameter, liquid flow rate and liquid inlet distributor configuration on the trickle-bed operation.

1.1 Structure of the Thesis

The thesis is organized as follows.

Chapter 2 gives a brief review of the literature reports on liquid flow texture, liquid distribution studies in trickle-bed reactors.

Chapter 3 presents the details of the model development.

Chapter 4 gives the detailed discussions on results.

Finally, conclusions are presented in Chapter 5.

CHAPTER 2

LITERATURE REVIEW

2.1 Introduction

The performance of trickle-bed reactors is influenced by hydrodynamics, mass transfer and reaction kinetics. The hydrodynamic parameters of importance are liquid distribution, liquid flow texture, pressure drop, liquid holdup, gas-liquid and liquid-solid interfacial areas. The effects of these parameters on the performance of trickle-bed reactors are rather complex and have been a subject of extensive research. Several excellent reviews on trickle-bed reactors have appeared from time to time in the literature: Satterfield (1975), Hofmann (1977), Gianetto et al. (1978), Shah (1979), Ramachandran and Chaudhari (1983), Herskowitz and Smith (1983), Dudukovic and Mills (1986), Gianetto and Silveston (1986), Gianetto and Specchia (1992), and Harold (1993). However, only those studies pertinent to the present work are briefly reviewed in this chapter.

2.2 Liquid Flow Texture

The various forms in which the liquid flows in the bed are collectively referred to as liquid flow texture. Depending upon the particle size and shape, the liquid texture in trickle-bed reactors may include films, rivulets, liquid pockets, pendular structures, and liquid filaments (Lutran et al., 1991). These flow features are depicted in Figure 2.1

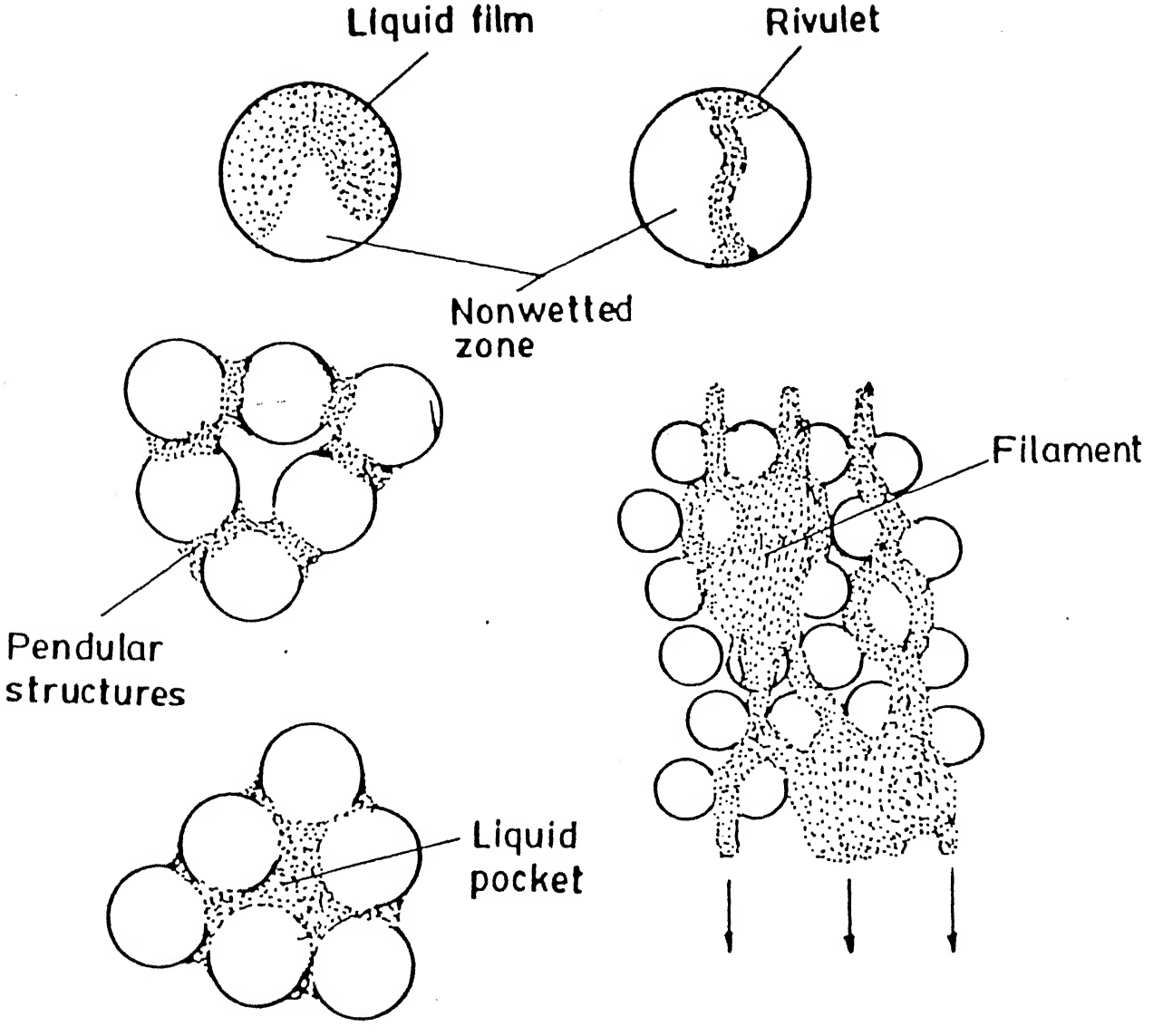

Fig. 2.1 Liquid flow texture in trickle-bed reactors
(Adapted from Lutran et al., 1991)

for spherical packing particles. Films and rivulets are associated with a single particle, while other flow features are associated with two or more particles. In film flow, the particles are fully or partially covered by the flowing liquid. In rivulet flow, the particles are partially covered by the flowing liquid. The pendular structures include pendular rings and liquid bridges. The former is formed at the contact points of the particles and the latter, when the particles are not in contact. The liquid pocket consists of the liquid entrapped between the particles. It can extend over several particles. The liquid filament is a continuous string of liquid pockets. Depending upon the particle size and liquid flow rate, these filaments may expand and form liquid channels. The above liquid texture may result in the formation of dry patches on particle-scale and bed-scale. The pressure drop, liquid holdup, gas-liquid and liquid-solid interfacial areas and reaction rates depend upon the extent of various flow features present in the reactor. Table 2.1 summarizes various studies on liquid flow texture in packed beds.

Christensen et al. (1986) observed the liquid texture at the wall for a large rectangular packed bed of 3 mm glass beads. Before the start of the run, they preflooded the bed with high gas and liquid flow rates and drained the liquid after terminating the flow of both the phases. They observed that the liquid flows in the form of channels when the liquid flow was gradually increased from zero flow rate to the preset value. However, they observed film flow at the same gas and liquid flow rates when the liquid flow rate was reduced from a higher value.

To understand the particle scale flow features, Melli et al. (1990) conducted experiments in a two-dimensional network which mimics the void space of packed beds. The bed was formed by circular rubber O-rings sandwiched between two transparent plastic plates. The rubber O-rings represent the solid particles. These were separated from one another to facilitate the visualization of the complete void space. Flow characteristics in the individual void spaces were recorded with a high speed video camera for various gas

Table 2.1 Studies on Liquid Flow Texture in Trickle-Bed Reactors

Reference	d_p (mm)	Packing Material	Startup Procedure
Christensen et al. (1986)	3.0	Glass beads	Prewetted & Drained
Melli et al. (1990)	7.0 & 9.0	Rubber O-rings	—
Lutran et al. (1991)	3.0 & 6.0	Glass beads	Prewetted
Tsochatzidis and Karabelas (1994)	6.0	Glass beads	Prewetted

and liquid flow rates. They observed trickling, bridged, flooded and bubbling flows in the void space between the particles and concluded that the flow regimes at the reactor scale are a result of microscopic flow characteristics at the particle level. However, the observed flow patterns were strongly affected by the presence of two flat walls, absence of particle-particle contacts and ordered packing.

Tsochatzidis and Karabelas (1994) employed a photography technique to record the flow patterns at the walls of a packed bed consisting of 6 mm glass beads. They observed gas-continuous, bridged, flooded, bubbling and dispersed bubbling flow patterns in the pore spaces. These flow patterns were similar to the ones as already reported by Melli et al. (1990) for the case of two-dimensional bed with O-rings. In trickling flow regime, they observed that the liquid is flowing mainly in the form of meandering liquid filaments. Isolated pendular structures, formed during the prewetting of the bed, were observed in the zones where the liquid was not flowing.

To explore the interior of the bed, Lutran et al. (1991) employed a Computer-Aided Tomography (CAT) technique. They studied the liquid texture in beds of glass beads with a quiescent gas phase. They observed a strong dependence of flow texture on whether the bed had been prewetted by flooding the column with liquid, or was initially dry. From the CAT-scans, they inferred that the liquid flows as films in case of prewetted beds, and as filaments in nonprewetted beds.

2.3 Liquid Distribution

The spatial distribution of liquid is expected to influence heat and mass transfer, and thus the rate of reaction. Distribution of liquid in the bed depends on the packing nature, shape and size, column diameter, gas and liquid flow rates, physical properties of liquid, and the type of inlet liquid distributor etc. There are several experimental and theoretical

studies reported in the literature on liquid distribution.

2.3.1 Experimental Investigations

Table 2.2 summarizes the experimental studies on liquid distribution in packed beds. Some of them are discussed below.

Weekman and Myers (1964) studied the radial liquid distribution for cocurrent, two-phase downflow through packed beds. They employed glass spheres (4.75 mm), and alumina spheres (6.48 mm). Three annular collectors were used to measure the outlet liquid distribution. They observed that most of the liquid flows through the central and wall regions of the bed. More uniform liquid distribution was observed at higher gas flow rates.

Herskowitz and Smith (1978) measured the liquid flow distribution at the bottom of the bed employing three to six annular collectors. They observed that the liquid distribution was uniform for aspect ratios greater than 18 for porous particles of 0.26 to 1.11 cm size. They found that the particle size and shape affected the liquid distribution. They proposed a theory to predict the liquid distribution. The model equations include a spreading factor and a wall factor. The former accounts for the fraction of liquid moving in the radial direction, and the latter for the wall flow.

Ahtchi-Ali and Pedersen (1986) passed nitric acid solution over the packing, comprising of 1.0 $\times$ 1.0 cm copper cylinders. The weight loss for every cylinder was noted. Considering that the weight loss of particle was proportional to its irrigation rate, they obtained the histograms of the particle irrigation rate. They found that the irrigation rate was not uniform in the bed. Based on the concepts of percolation theory, a model was proposed for the simulation of liquid flow patterns.

Marchot et al. (1992a) measured the liquid flow distribution in a laboratory trickling

Table 2.2 Experimental Studies on Liquid Distribution in Packed Beds

Reference	d_p (mm)	Packing Material	Startup	Liquid Collector
Weekman and Myers (1964)	4.75 & 6.48	Glass beads and Alumina particles	—	3 annular rings
Sylvester and Pitayagulsarn (1975)	3.2 × 3.2	Cylinders	—	6 annular rings
Prchlik et al. (1975)	9.0 × 7.2	Nickel on Kieselguhr	Prewetted	13 annular rings
Herskowitz and Smith (1978)	2.58-11.1	Porous particles	Prewetted	3 to 6 annular rings
Ahtchi-Ali and Pedersen (1986)	10 × 10	Copper cylinders	—	Loss in weight of each cylinder
Marchot et al. (1992a)	50×30 to 187×50	Polymeric cylinders	—	441 sampling sections
Ravindra., (1995)	1.6, 3.5, 5.7 & 6.3	Glass beads and Alumina particles	Preewtted & Nonprewetted	Annular collector with 16 partitions

filter, packed with cylinders of polymeric material of 5.0 × 3.0 cm. The histograms for fraction of the cross-sectional area receiving different liquid flow rates were obtained. The histograms revealed that about half the bed cross-section did not receive any liquid, and the flow rate distribution was not uniform in the rest of the bed cross-section. They also proposed a theory based on the concepts of percolation theory to predict the observed liquid flow distribution.

Ravindra., (1995) measured the exit liquid flow distribution at the bottom of the bed employing a collection device with 16 partitions. Point, line and uniform inlet configurations have been used in his study. An interesting feature of this study is complete wetting of particles. He has conducted experiments with nonprewetted and prewetted startup procedures and studied exit flow distributions with point, line and uniform inlets. With nonprewetted bed, channelling and bed-scale partial wetting was observed by him. However, with prewetted bed, he has observed complete wetting of the bed with point, line and uniform inlets. The results of this study by Ravindra (1995) are discussed in detail in chapter 4 since the results obtained through simulations in the present study are compared with these results.

2.3.2 Theoretical Investigations

In the literature, three approaches have been used to model the liquid flow in trickle-bed reactors. These are diffusion models, models based on percolation theory, and models that make use of computer-generated sphere packs. The details of these models are presented in this section.

In the diffusion models, it is assumed that the packing is a homogeneous medium. The radial spreading of liquid is then assumed to be governed by a diffusional mechanism, and described by the equation

$$\frac{\partial f_w}{\partial z} = \frac{D_r}{2} \nabla^2 f_w \tag{2.1}$$

where D_r is a coefficient of radial spread of the liquid, f_w is the local flow mean density and z is the axial bed coordinate. For an initial point source distribution, this implies that the local liquid flow density is a Gaussian function of the radial displacement. Liquid distributors of different configurations were readily simulated with this model. This approach was followed by numerous workers: Tour and Lerman (1944), Cihla and Schmidt (1957), Stanek and Kolar (1973), Stanek et al. (1981), among others. However, the diffusion model has a weak point. In this model, the liquid propagates indefinitely, which is not realistic because radial spreading is observed to cease when the axial flow rate is sufficiently low.

To account for the liquid flow in preferential paths (Bemer and Zuiderweg, 1978), and the discontinuous nature of the medium, models based on percolation theory have been proposed. These models were further developed by Crine et al. (1979, 1980) and Marchot et al. (1992a, 1992b) to simulate the liquid flow patterns. In this methodology, the medium is represented by a three-dimensional lattice, the bonds of which simulate the connections between the transport cells. Hydrodynamical connection (active property) is assigned to each transport cell following some stochastic distribution. The flow structures obtained by this method depend strongly upon the boundary conditions at the lattice edge wall, the type of initial liquid distribution, and the lateral lattice wall effect.

In sphere pack models, a computer-generated column packed with spheres is used to represent the topology of the bed, which serves as the framework on which liquid flow takes place. A large number of studies on computer generated sphere packs have appeared on the literature. Table 2.3 gives brief summary of the works reported in the literature. The procedure used to form a sphere pack varied among different investigators. Adams and Matheson (1972), Bennett (1972), Matheson (1974) and Powell (1980) placed

Table 2.3 Summary of literature on computer generated sphere packs

Authors/Year	Procedure	Geometric characterstics
Adams and Matheson (1972)	Spheres are sequentially added to triangular sites on the surface of an existing spherical cluster of spheres	Packing density; Radial distribution function
Bennett (1972)	Ditto	Coordination number; Radial distribution function
Visscher and Bolsterli (1972)	Spheres are sequentially added to a three-dimensional box without rigid walls	Packing density; Radial distribution function
Tory et al. (1973)	Ditto	Porosity; Distribution of circle diameters in a sectional cut; Radial distribution function
Matheson (1974)	Spheres are sequentially added to triangular sites on the two circular ends of an existing cylindrical cluster of spheres	Packing density; Coordination number; Radial distribution function
Powell (1980)	Spheres are sequentially added to a three-dimensional box with no rigid walls and no base	Packing desity; Coordination number

spheres one at a time in contact with three spheres of an existing sphere pack. Visscher and Bolsterli (1972) and Tory et al. (1973) dropped spheres sequentially onto a heap of spheres. Every sphere was allowed to roll under gravity until it settles down to a stable position.

After generating the sphere pack, an inlet liquid distribution with a specified configuration is imposed at the top of the bed. The liquid that enters the sphere pack is considered to spread out from sphere to sphere through the contact points. The advantage of this approach over percolation theory, which utilizes a network with specified interconnectivity, is that the spatial variation of the coordination number is accurately reproduced. Zimmerman and Ng (1986), Zimmerman et al. (1987) and Funk et al. (1990) employed this approach to generate flow distributions for different liquid inlet configurations. However, they have employed a two dimensional computer generated sphere pack for their study. A two dimensional model does not represent actual three dimensional bed. The co-ordination number of three dimensional pack i.e the number of spheres in touch with a given sphere, is about six (Chan and Ng, 1986) and can even be more whereas it is four in their study. Their other assumption is that the flow rate that a sphere receives gets equally distributed among the spheres which are touching it below the equator. This may not be correct because the amount that a sphere receives from top sphere depends on the angle of contact.

A model is developed which uses a three dimensional packed bed to represent the porous medium needed for the study. Thus the co-ordination number is exactly represented. Flow distribution of liquid among the spheres takes into account the orientation of contact as greater amount of liquid is supposed to go to the particle which is at a steeper angle from the equator. Other features of the model will be discussed in detail in the next chapter.

CHAPTER 3

MODEL DEVELOPMENT

3.1 Introduction

A schematic diagram of a typical trickle-bed reactor is shown in Figure 3.1. It consists of a liquid distributor, packed bed section and a gas-liquid separator. Gas and liquid flow cocurrently down the reactor through the packed bed. The liquid distributor can be configured for different inlet conditions.

The three approaches to model liquid distribution in trickle-bed reactors is been discussed in section 2.3.2. In this study a sphere pack based model has been developed. Prior to this, Zimmerman et al. (1986) have used 2-dimensional sphere pack to simulate the flow distribution. In the present study, flow distribution is simulated using a 3-dimensional sphere pack. The model can be divided into two parts. one, a porous medium model to account for the interactions between the fluid and the solid matrix. Other, a liquid flow pattern is generated through flow simulation.

3.2 Porous medium model

A three dimensional computer generated bed packed with equal-sized spheres serves as the porous medium. For the present study, *PACKS3*, a C language program developed

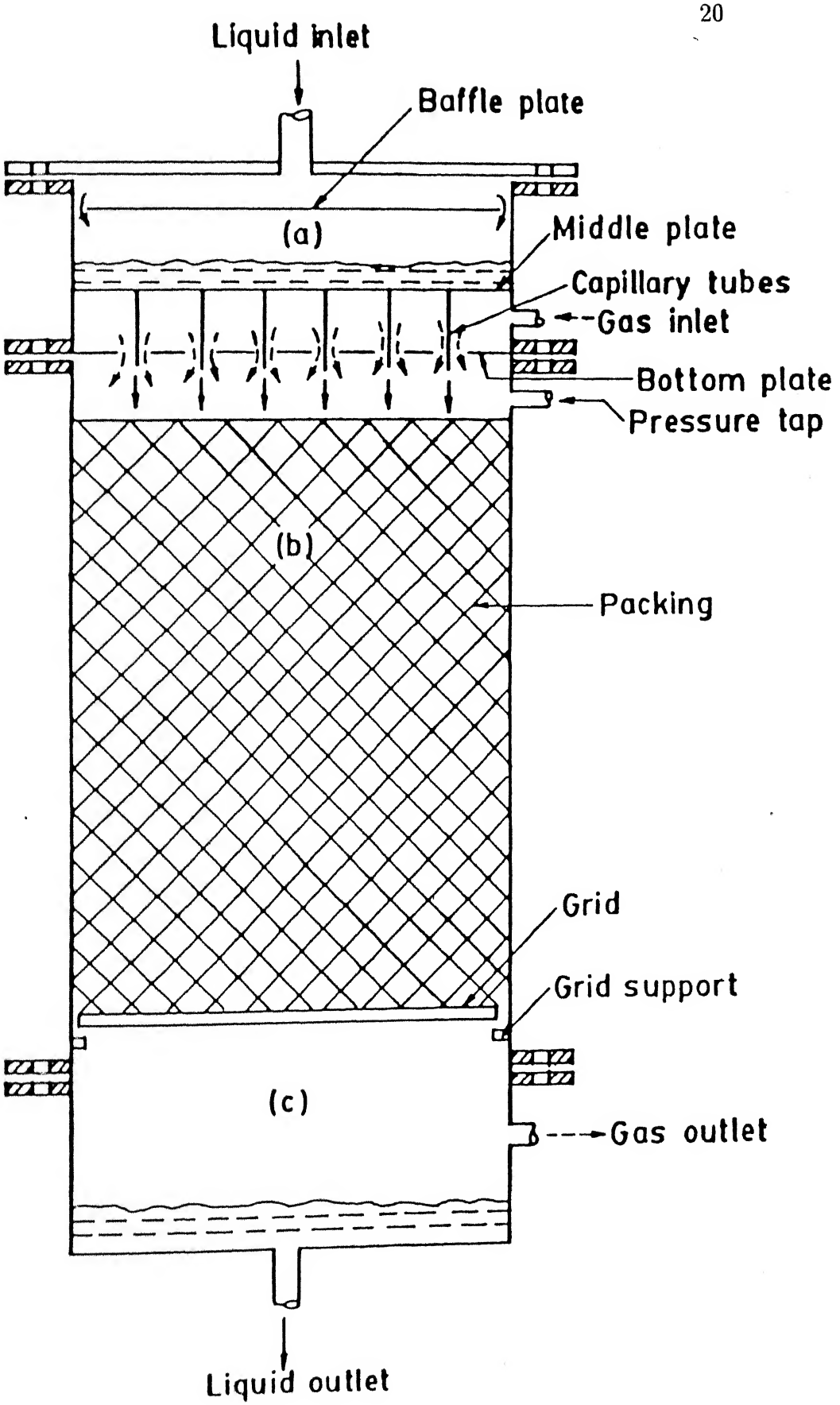

Fig. 3.1 Schematic diagram of the trickle-bed reactor
(Adapted from Ravindra., 1995)

by Monica Bargeil., (1990)(based on the algorithm proposed by Jordey et al. (1979)), to simulate a three dimensional packed bed, is used to generate the porous medium.

PACKS3 describes the slow settling of rigid spheres from a dilute suspension into a randomly generated packed bed. Settling takes place in a semi-infinite box defined by: { x, y, z — $0 \leq x \leq w$, $0 \leq y \leq w$, $z \geq 0$ }. Periodic boundary conditions with complete continuity at the boundaries has been used. This yields a packing which is effectively infinite in xy-plane. Rough floor reduces the disturbance at the bottom. Since the distribution of spheres in a dilute settling slurry is random, the simulation assumes that the initial x and y co ordinates are chosen according to the probability density function (*p.d.f*)

$$g(x,y) = f(x)f(y) \tag{3.1}$$

$$\text{where } f(x) = 1/w \quad 0 < x < w \tag{3.2}$$

$$= 0 \qquad \text{elsewhere} \tag{3.3}$$

and f(y) is also similarly defined.

Each sphere is introduced above the bed in a potential field $\phi(z)$ in which $\phi(0) = 0$ and $\phi'(z) > 0$ for $z \geq 0$. In seeking the position of minimum potential, a sphere may roll off others but is prohibited from any movement even infinitesimal which would increase its potential. Subject to the appropriate constraints, a sphere follows a path along which the potential gradient is maximum. Each sphere progresses through a series of discrete events. For example, a sphere may hit another, roll on it until a second sphere is struck, and roll on both the spheres until a third sphere is hit. In this case, the events are hits. The equations specifying a particular hit are solved analytically and the height at which an event would occur is compared to the height at which other events would occur. The event which would happen first is the one which is presumed to occur. The only events are hits (on spheres or floor) and roll-offs. A sphere is stable when any roll would increase its potential. Any sphere which touches the floor is considered to be stable. To ensure that the spheres which hit the bottom of the box do not pack regularly, the

position of the box is varied for each sphere according to the probability density function $(p.d.f)$

$$f(z) = 1/2 \quad 0 < z < 2 \tag{3.4}$$

$$= 0 \quad \text{elsewhere} \tag{3.5}$$

However, these spheres occupy unique positions and spheres on or near the floor are excluded from all (characteristics) calculations of packing characteristics.

Each sphere in the simulation is introduced only after the previous one is permanently in place. Because the spheres creep, the simulation assumes no bouncing, no bumping of precariously stable spheres to more stable positions and no consolidation by spreading of spheres apart to accommodate incoming spheres.

All these features make a greater proportion of simulated spheres truly random in final position and as available for analysis. Preservation of addresses of supporting spheres simplifies the subsequent analysis for nearest neighbours.

3.3 Flow Simulation

Liquid enters the sphere pack from inlet tubes positioned at different locations. The simulation procedure takes advantage of the fact that liquid flows from particle to particle down the bed and thus the flow information concerning the particles is also from top to bottom of the reactor. The absence of back mixing allows the examination of flow on each pellet, one at a time, until all the pellets in the bed are considered. The flow rate from each inlet tube can be prespecified.

3.3.1 Liquid Spreading

Consider the following situation: A laminar thin film of liquid flows down a vertical wall. The liquid rate is not enough and a dry spot is formed (Fig. 3.2). At the stagnation point the liquid changes its direction and its kinetic energy is converted into stagnation

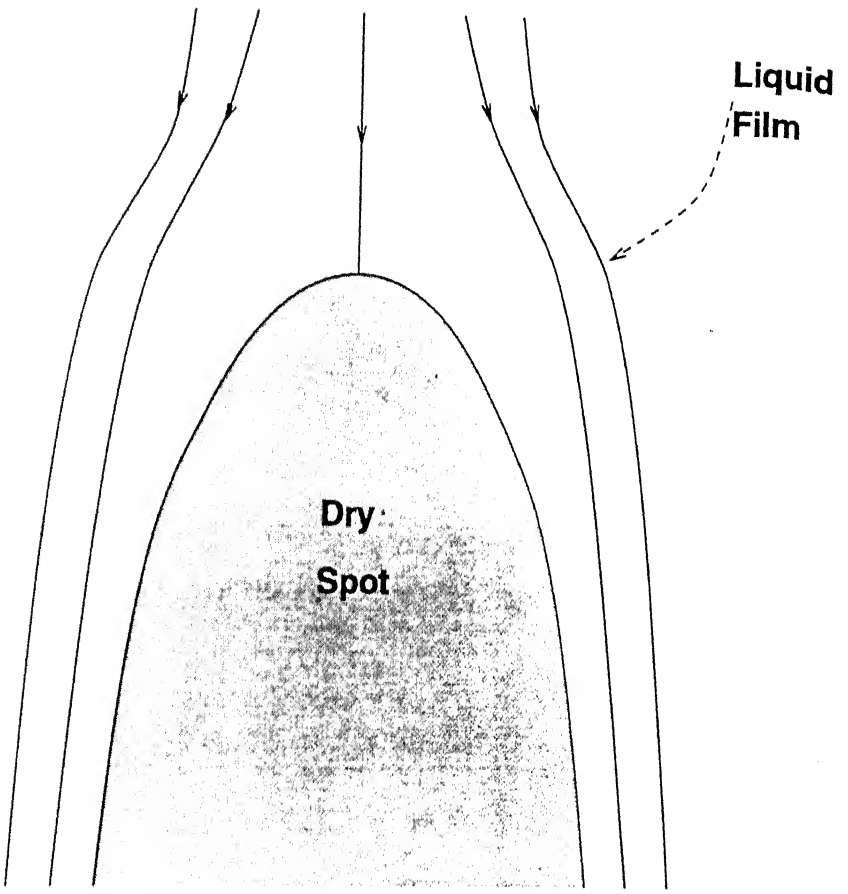

Fig. 3.2 Dry patch model
(Adapted from Hartley and Murgatroyd., 1964)

force that tends to push the contact line downward. The contact line is still pinned on the wall because of the surface tension force.

Based on this Dry patch model described above, Hartley and Murgatroyd (1964) suggested that the minimum flow rate per unit length, m, above which the stagnation force is always greater than the surface tension effect is proportional to the physical properties of the system in the following manner.

$$m \propto \left(\frac{\mu\rho}{g}\right)^{1/5} \sigma^{3/5} \tag{3.6}$$

The experimental data of Norman and McIntyre (1960) indicate that the proportionality constant is of the order of 0.1. Here μ and ρ are viscosity and density of liquid respectively. g is acceleration due to gravity and σ is interfacial tension.

$$\text{Thus} \quad m = 0.1 \left(\frac{\mu\rho}{g}\right)^{1/5} \sigma^{3/5} \tag{3.7}$$

Applying this concept to the packed bed, the minimum superficial mass flow rate of liquid L_{min}, to attain complete wetting can be estimated by multiplying flow rate per unit length, m, with the total length of the grain boundary per unit cross sectional area, S.

$$\text{Hence} \qquad L_{min} = m.S \tag{3.8}$$

For a spherical particle, the minimum volumetric flow rate, q_c, required to wet it completely is given by the expression :

$$q_c = \pi d_p 0.1 \left(\frac{\mu\rho}{g}\right)^{1/5} \left(\frac{\sigma^{3/5}}{\rho}\right) \tag{3.9}$$

3.3.2 Flow distribution among packings

Consider a case where a parent sphere has three daughter spheres. Daughter spheres here imply that those spheres touch the reference or the parent sphere below equator. Let q_t

be the amount of flow rate that the parent sphere receives. Let θ_1, θ_2, θ_3 be the contact angles made by the daughter spheres with the parent sphere at the equator respectively. It is assumed that the liquid flow from the parent sphere to the daughter spheres is a function of orientation of contact and relative orientations of other daughter spheres. In simple terms, $q_i = f(\theta)$. It can be written as:

$$q_1 = \left(\frac{q_t \sin\theta_1}{\sum \sin\theta}\right) \tag{3.10}$$

$$q_2 = \left(\frac{q_t \sin\theta_2}{\sum \sin\theta}\right) \tag{3.11}$$

$$q_3 = \left(\frac{q_t \sin\theta_3}{\sum \sin\theta}\right) \tag{3.12}$$

$$\text{where} \quad \sum \sin\theta = \sin\theta_1 + \sin\theta_2 + \sin\theta_3 \tag{3.13}$$

Two subsets of flow distribution criteria has been used. one for the prewetted bed case and the other for nonprewetted bed case.

For **Nonprewetted bed** case, the distribution criteria is as follows. The liquid from the parent sphere is distributed to daughter spheres as per the distribution function described above. It was assumed that the particle which receives an amount less than q_c *(critical flow rate required for complete wetting)* does not receive liquid at all. If none of the daughter spheres receive an amount greater than q_c, the daughter sphere with maximum contact angle with the parent sphere gets the liquid.

However, for the **prewetted bed** case, since a liquid film already surrounds the particle, the question of critical flow rate for complete wetting does not arise. Thus, the flow rate that a parent sphere receives gets distributed among daughter spheres according to the distribution function mentioned above.

3.3.3 Flow Simulation Algorithm

One key advantage of the simulation approach to study liquid distribution in trickle-beds is that all the system variables - packing diameter, liquid flow rate, surface tension, liquid

distributor configuration etc... can be readily and independently controlled.
In particular, the liquid distributor configuration determines whether the liquid feed at the top of the column is uniform or line or point or selective.
After further specifying the physical properties of the system such as liquid density, viscosity and surface tension the simulation algorithm described below is followed.
(1) Specify the locations or type of inlet configuration and liquid flow rates.
(2) Determine the amount of liquid a sphere receives if any, from the liquid distributor. Of course, the input liquid primarily goes to those spheres which are on the top of the bed.
(3) Starting from the highest sphere in the bed, sum all the liquid flow rates from higher spheres that are in contact with the current sphere and / or from the liquid distributor.
(4) Identify the spheres below and in contact with the current sphere.
(5) Determine liquid flow rates at the various outlets of the current sphere.
(6) Distribute the liquid among the daughter spheres using the criteria described above for different cases of nonprewetted and prewetted bed.
(7) Return to the step 3 for next highest sphere and continue till all the spheres in the column are considered.

Thus the liquid works its way down the column. The outlet flow streams calculated for spheres at one layer becomes the inlet streams for next level of packing. As the volume balance calculations proceed down the bed, the liquid flow distributions for the various spheres are determined.

CHAPTER 4

RESULTS AND DISCUSSIONS

4.1 Introduction

Flow maldistributions in trickle bed reactors has been a challenging problem for investigators since a long time. Some of the studies in this area are discussed in detail in chapter 2. In a recent study, Ravindra (1995), employed a dye-adsorption technique to examine the particle scale and bed-scale features of the liquid flow texture. The study involved flow distribution measurements for beds of porous and nonporous particles with nonprewetted and prewetted startup procedures. One salient feature of his study is complete wetting for particle size less than 5.7 mm for nonporous particles (glass beads) and 6.3 mm for porous particles (alumina particles). Based on this observation, a model has been proposed for flow distribution in chapter 3. This chapter deals with results of flow distribution simulations.

Before discussing the results of simulations, the experimental findings of Ravindra (1995), related to the present study are briefly presented below.

4.2 Previous Experimental Observations :

This section deals with brief review of experimental observations of Ravindra (1995) whose results will be compared with those obtained by flow simulations. The bed em-

ployed in his study was rectangular in cross-section with inner dimensions of 6.0 × 8.0 cm and a height of 20 cm. In order to distribute liquid over the packing, *uniform, line* and *point* inlets were used in his study. A *uniform inlet* consisted of 99 stainless steel capillary tubes and *line inlet* has nine capillary tubes. A dye adsorption technique was adopted and flow texture was inferred by taking pictures at different cross-sections.

Figure 4.1 shows the schematic diagram of collection device used to study exit liquid flow distribution from the trickle-bed reactor. The interior of the device was partitioned into 16 equal sized rectangular cells. Flow rates in various cells have been determined and percentage liquid distribution is calculated by dividing the flow rates in each cell by the total liquid flow rate. The standard deviation (SD) which is a measure of deviation from uniform liquid flow through cells has been calculated. The observations of liquid flow distribution are presented in the following subsections, for nonprewetted and prewetted beds employing point, line, and uniform-liquid inlets.

4.2.1 Point Inlet

Nonprewetted Bed :

With glass beads of 1.6 mm size, only a single liquid channel was formed. The visual observations and photographs taken at different cross sections by Ravindra (1995) (not shown here) indicate that the particles located inside the channel were completely colored and the ones outside the channel appeared bone-dry. Partially wet particles were not observed even at the interface of the channels and dry zones. The liquid flow rates through the cells are shown in Figure 4.2(a). It can be seen from the Figure that the middle cells (6,7 and 10,11) are particularly active.

Prewetted Bed:

The behavior of prewetted beds of glass beads with point inlet was strikingly different from that of nonprewetted beds. It was observed that the particles at all the other

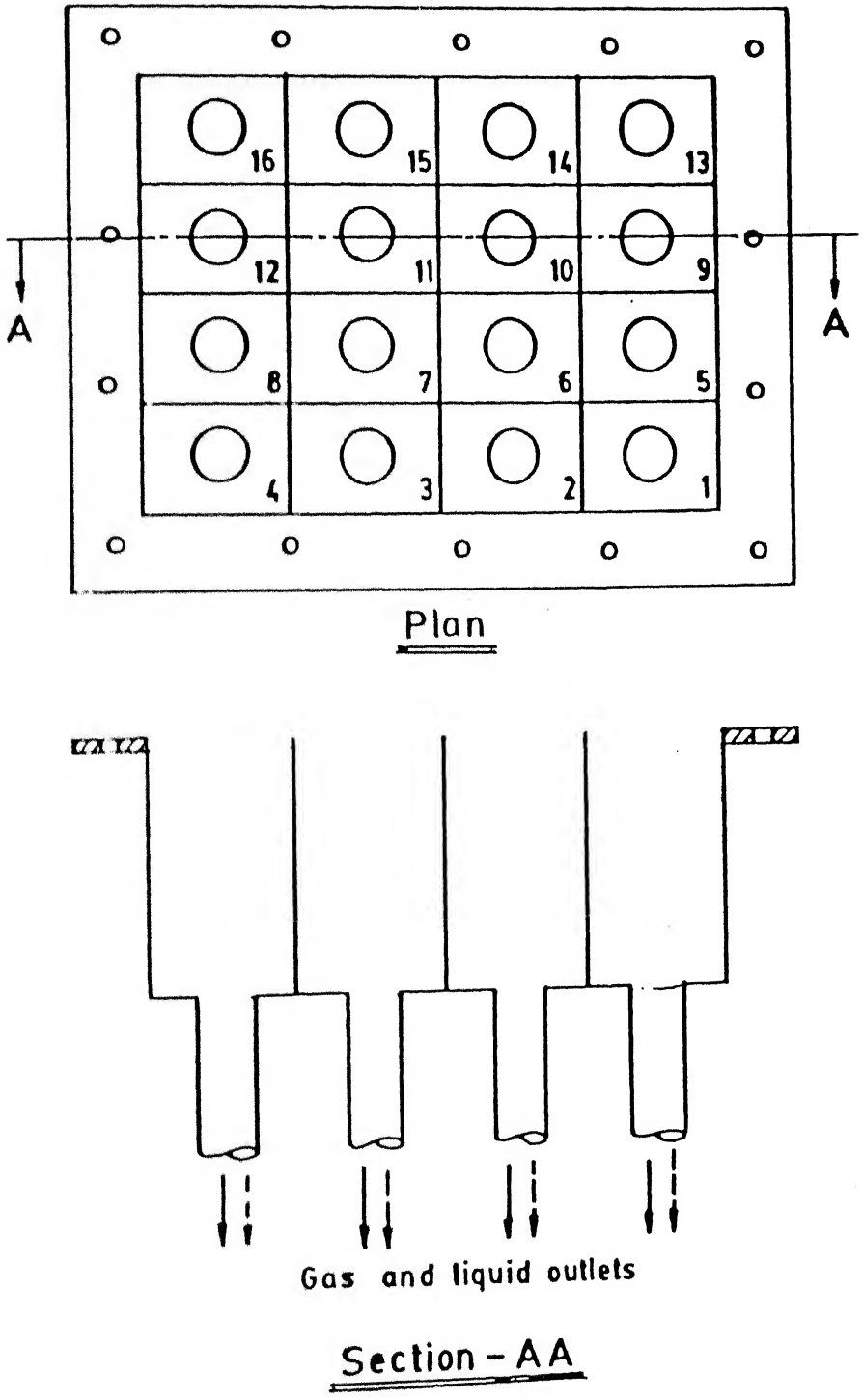

Fig. 4.1 Schematic diagram of liquid collection device used by Ravindra., (1995)
(cells are identified by numbers given in the right corner)

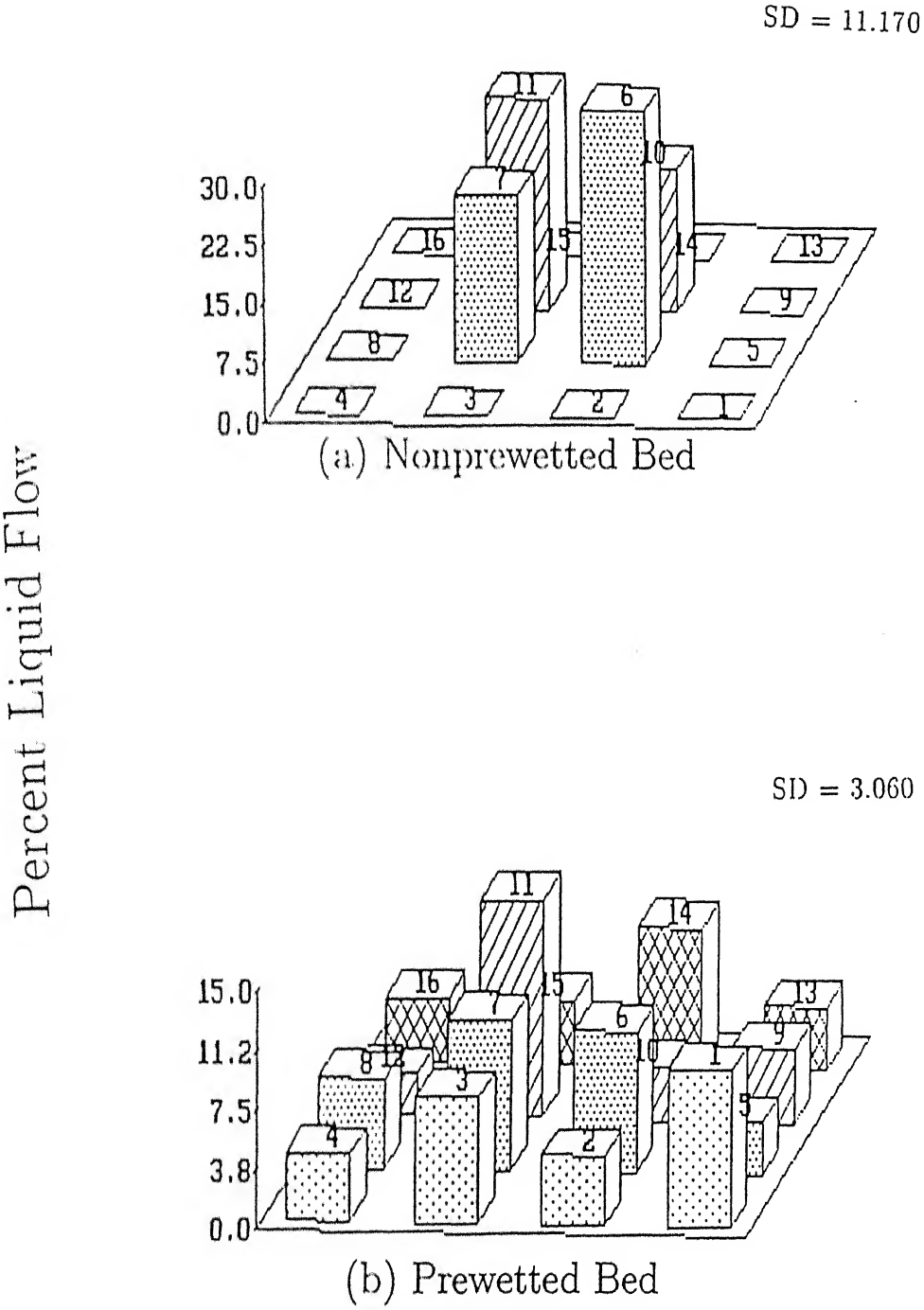

Fig. 4.2 Exit liquid flow distribution with Point Inlet distributor

cross-sections were completely wet. Figure 4.2(b) shows the exit liquid distribution in a prewetted bed point inlet. Exit flow distributions show that all the cells of collection device are active and those cells around the inlet liquid distributor position receive much of the liquid flow.

4.2.2 Line Inlet

Nonprewetted Bed:

For a nonprewetted bed of 1.6mm glass beads when the liquid is distributed by *line inlet* it was observed that a liquid channel with a rectangular cross section was formed at the top of the bed. The particles in the dry zone were observed to be bone dry and the ones inside the channel were completely wet. The liquid distribution is shown in Figure 4.3(a). The cells in the two columns at the middle were active. Severe maldistribution of liquid was there among the cells.

Prewetted Bed:

The texture of prewetted bed with line inlet was similar to that with point inlet. Barring a few particles in the top layer, all the particles at all the cross sections were wetted completely. The exit liquid distributions in prewetted beds of glass beads with line inlet are shown in Figure 4.3(b). The discharge rates through the cells in the middle rows were higher compared to the outer ones. The liquid distribution is more uniform in prewetted beds than in nonprewetted beds.

4.2.3 Uniform Inlet

Nonprewetted Bed:

The exit distribution of liquid from nonprewetted bed with uniform inlet is shown in Figure 4.4(a). Ravindra (1995) has taken pictures of different cross sections of the bed and has observed formation of distinct channels at about 3 cm depth from top. These

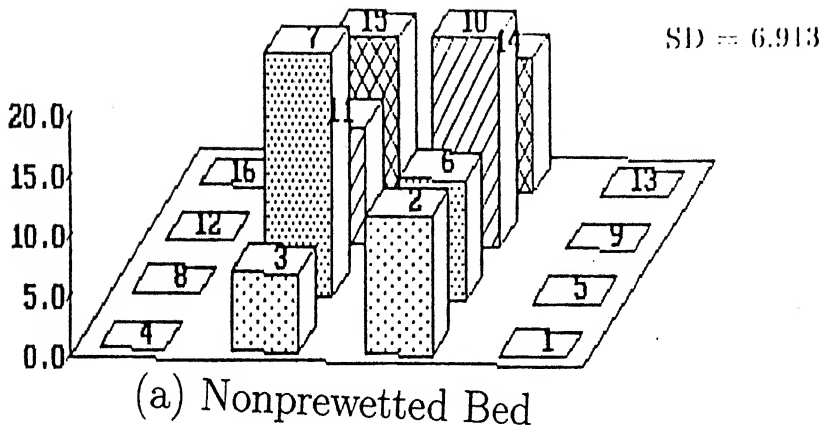

Percent Liquid Flow

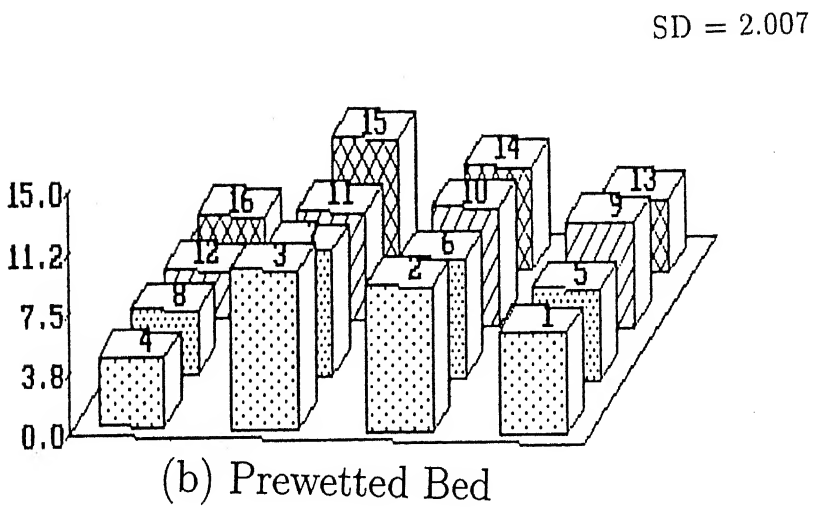

Fig. 4.3 Exit liquid flow distribution with Line Inlet distributor
$d_p = 1.6\,mm$, $L = 1\ kg/m^2.s$, Bed size : $60 \times 80 \times 200\,mm$
a : Nonprewetted bed b : Prewetted bed
(Adapted from Ravindra., 1995)

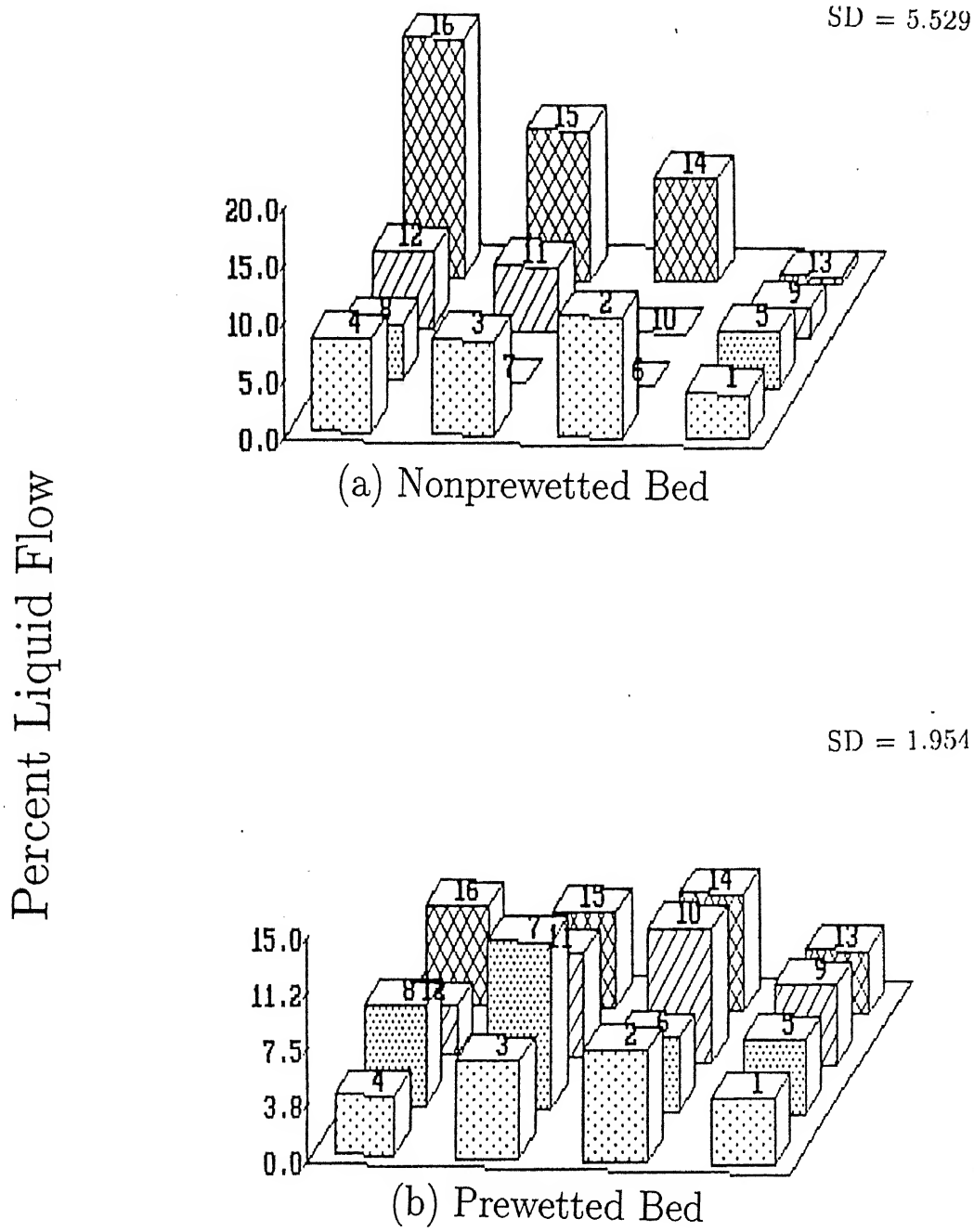

Fig. 4.4 Exit liquid flow distribution with Uniform Inlet distributor
d_p = 1.6 mm, L = 1 kg/m^2.s, Bed size : 60 × 80 × 200 mm
a : Nonprewetted bed b : Prewetted bed
(Adapted from Ravindra., 1995)

channels meandered, merged and split with depth. The particles in the colored zones were completely wet whereas those in the noncolored zones were bone dry. No particle-scale partial wetting was observed.

Prewetted Bed:

Figure 4.4(b) shows the exit liquid distribution in the case of *prewetted bed* with *uniform inlet.* All the particles were completely wetted with the liquid and also the liquid was distributed throughout the bed.

To summarize, channel flow was observed in nonprewetted beds of glass beads at low liquid flow rates. The number of channels and the channel width varied depending on the particle size and the type of liquid inlet distributor employed. Particles located inside the channels were completely wet and the ones outside were bone-dry. As the liquid rate was increased, the channels enlarged. *Bed scale partial wetting* which was observed at low liquid flow rates decreased with increase in liquid flow rate. In contrast, in prewetted beds of glass beads, *complete wetting* of both the particles and the bed was observed at a liquid velocity as low as 1.0 $kg/m^2.s$ for all the three liquid inlet configurations. It was also observed that increase in liquid flow rate has least effect on the distribution of liquid in case of prewetted beds.

The models available in the literature for liquid distribution, appear to be inadequate to predict some of the features observed in this study by Ravindra (1995) like, complete wetting of the prewetted bed with point inlet, channel flow in nonprewetted beds with uniform inlet distribution, and some other features.

4.3 Theoretical Simulations

This section deals with discussions on some selected results. Three-dimensional packed bed needed for the study has been generated using a C language program by Monica Bargeil (1990) (based on the algorithm proposed by Jordey et al., (1979)). Packed beds of different dimensions are simulated and exit flow distributions are checked for different inputs. Water is taken as the liquid under consideration and the physical properties of water at 35 °C are used for the calculations. The results obtained through simulations are compared with those of experimental results for nonporous particles whereever the situation seems similar.

The sphere pack program used to generate three-dimensional packed beds has two constraints. One, it produces a packed bed which is square in cross section. Other, the minimum particle diameter for which it generates a packed bed is 2.0 mm. However, a rectangular (60 × 80 mm) bed has been used by Ravindra (1995) to carry out flow distribution experimnts. As the beds differ in shapes, comparison of results is more of qualitative nature.

The effect of inlet distributor configuration, liquid flow rate and diameter of the particle are discussed in the coming subsections.

4.3.1 Configuration

Ravindra (1995) conducted two sets of experiments with nonporous particles to study the effect of configuration on exit liquid distribution. One, with 1.6 mm diameter particles using point, line and uniform inlets. Other, with 3.5 mm and 5.7 mm particles using uniform inlet.

As the minimum diameter that can be taken to generate a sphere pack is 2.0 mm, a bed with 40 × 40 mm and height 45.23 mm has been simulated with 9000 spheres of 2.0 mm diameter and the flow has been simulated for point, line and uniform inlets.

Given below is detailed discussion.

4.3.1.1 Nonprewetted bed

Point inlet :

A point inlet is placed at (20.0,20.0) on the xy-plane at the top of the reactor. A typical picture of point inlet is shown in Figure 4.5(a). Liquid enters at a flow rate of 1 $kg/m^2.s$. It will primarily go to the particle on top. The exit distribution through the cells is shown in Figure 4.6(a) as 3-dimensional histograms. It can be observed that cells 6,7,10 and 11 are active and rest of the cells does not receive any liquid. This could be compared with the channel formation observed in the case of nonprewetted bed with point inlet by Ravindra (1995). In his case also the exit liquid distribution showed that only the cells surrounding the inlet liquid distributor position are active (Fig. 4.2(a)).

Line inlet :

For the same bed dimensions of 40 mm × 40 mm × 45.23 mm a line inlet is used at nine different positions across the y axis. A typical picture of the line inlet is shown in Figure 4.5(b). The x co-ordinate is 20.0 for all the input points where as y co-ordinate varies from 4.0 to 36.0. An input liquid flow rate of 1 $kg/m^2.s$ has been used for the simulation and it has been distributed equally among all the inlet points i.e each inlet point receives a flow rate equal to 1/9 of total flow rate.

The exit liquid distribution from the Figure 4.6(b) shows that the cells in the middle row are particularly active and the cells in the other rows do not receive any liquid. It can also be seen that some of the cells in the middle rows like cells numbered 14 and 15 does not receive liquid. It can be interpreted as channel formation which was observed by Ravindra (1995) in the case of nonprewetted bed with line inlet (Fig. 4.3(a)).

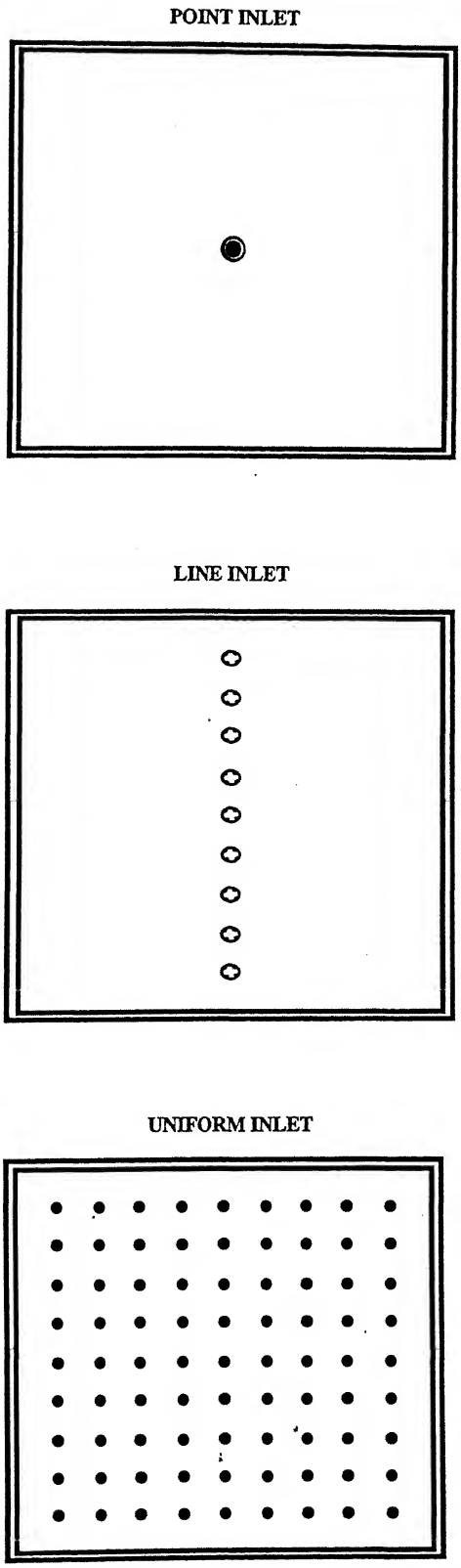

Fig. 4.6 Model diagram of Inlet Distributor Configuration
a : Point Inlet b : Line Inlet c : Uniform Inlet

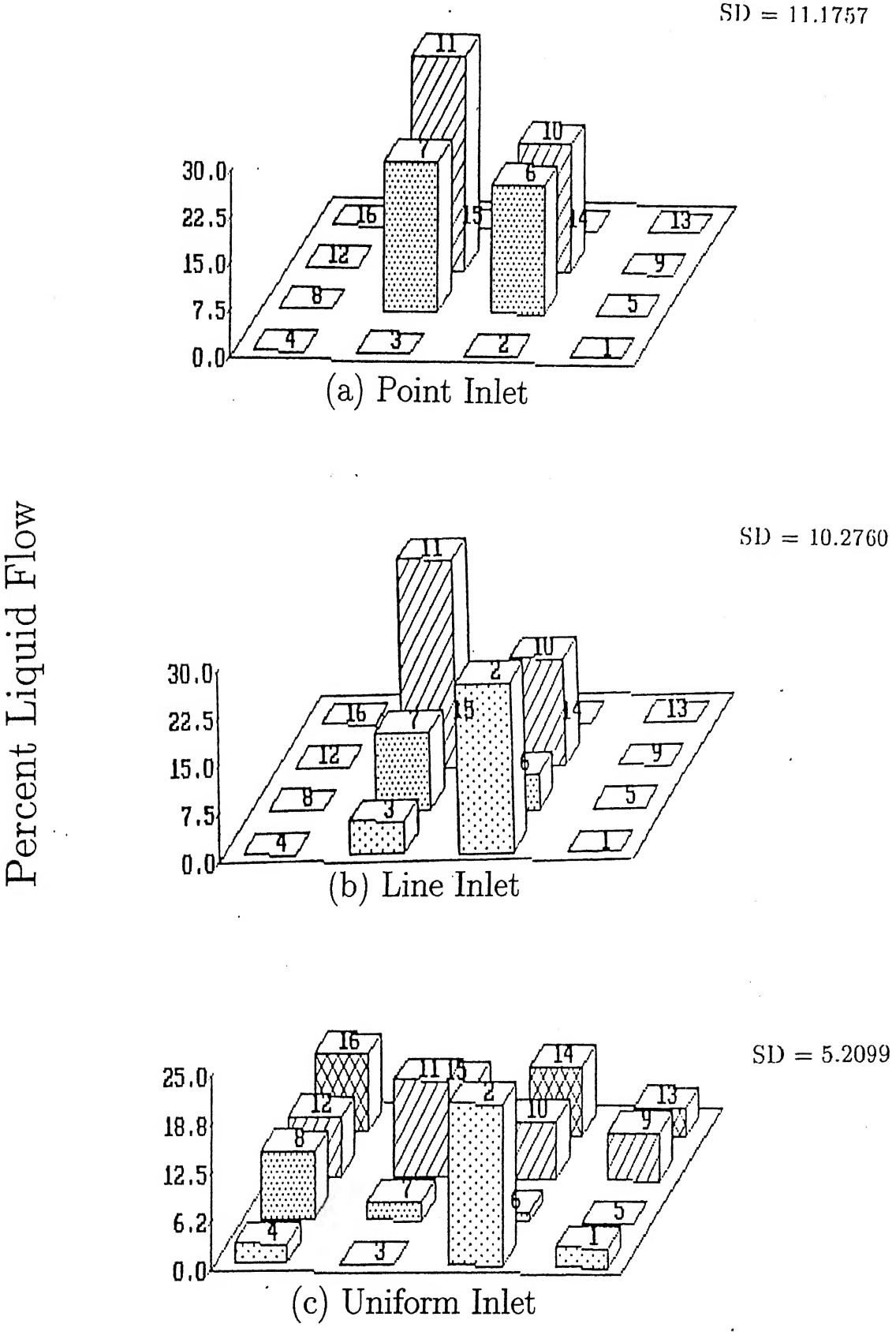

Fig. 4.6 Exit liquid flow distribution in Nonprewetted beds

Uniform inlet :

Figure 4.5(c) gives the typical view of uniform inlet. It consists of 81 inlet positions which are distributed across the bed uniformly. The inlet flow rate is $1\,kg/m^2.s$. In this case, each inlet point receives 1/81 of the total input liquid flow rate.

Figure 4.6(c) shows exit distributions through different cells. It can be observed that the cells 3 and 5 do not receive any liquid. Maximum amount of flow has been received by the cell 2. This can be compared with the Figure 4.4(a) which depicts a similar experimental situation. Inactive cellls (3 and 5) may refer to the maldistribution due to channel formation which was observed experimentally (Fig. 4.4(a)).

4.3.1.2 Prewetted bed

Point inlet :

A bed with same dimensions ($40 \times 40 \times 45.23\,mm$) as in the case of nonprewetted bed is used to study the exit flow distributions. Fig. 4.7(a) shows the exit flow distribution of percentage liquid flowing out from different cells for the case of prewetted bed with point inlet. It can be seen that all the cells receive liquid and the cells in the middle receive much of the flow. Figure 4.2(b) gives the distribution profile observed experimentally. Comparison of Figures 4.2(b) and Figure 4.7(a) shows that there is variation in the percentage of liquid received by the middle cells and the cells at the walls. However, this can be attributed to small size of the bed taken for simulating the flow. To check this, a bed of $40 \times 40 \times 94.63\,mm$ is simulated and exit flow distribution is depicted as Figure 4.8(a). It can be observed that the percent flow received by cells at the walls is increased. This result may imply a close experimental behaviour with similar bed dimensions.

Line Inlet:

Figures 4.7(b) and 4.8(b) show the exit flow distributions from different cells of the beds with dimensions $40 \times 40 \times 45.23\,mm$ and $40 \times 40 \times 94.63\,mm$ respectively. It

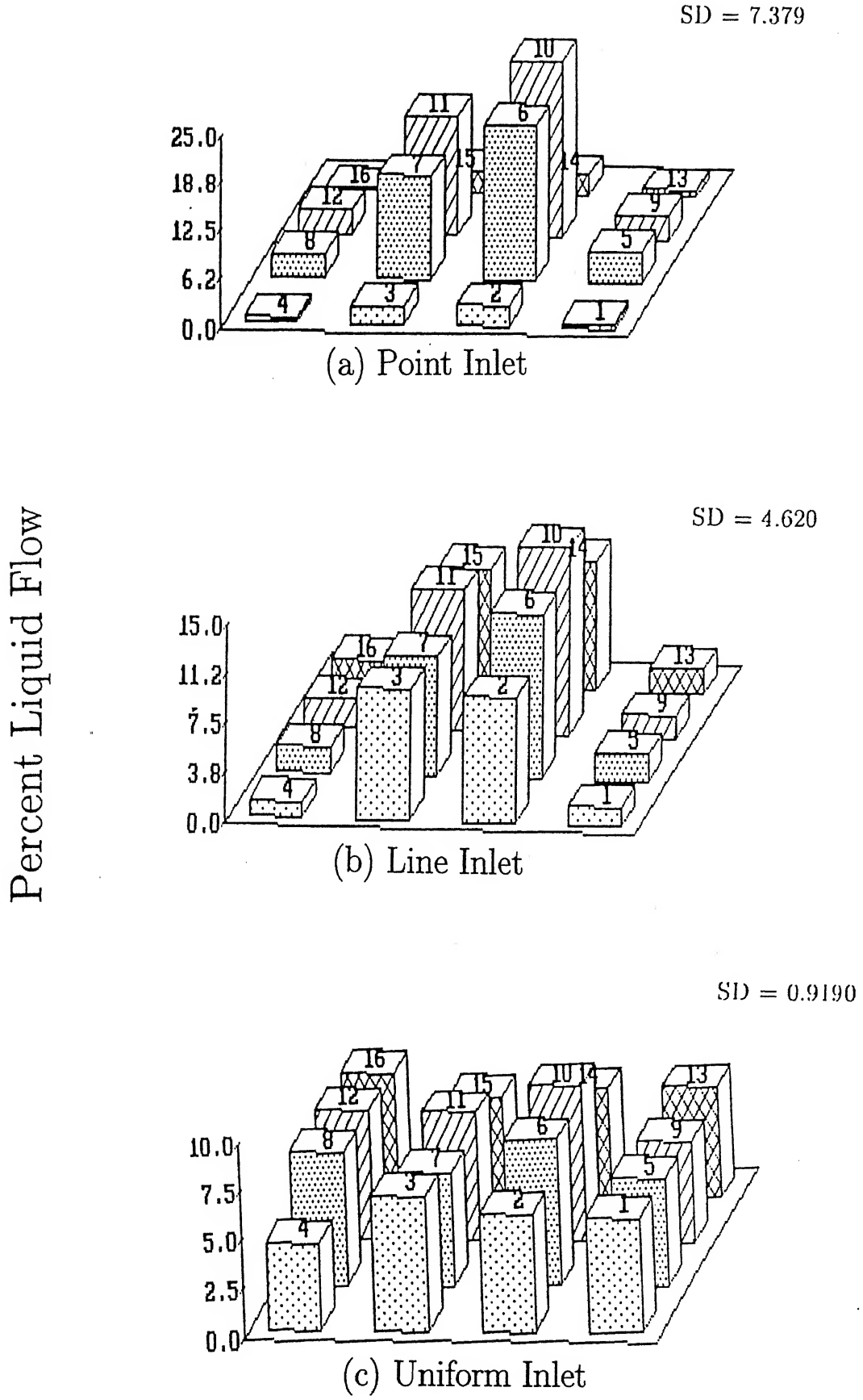

Fig. 4.7 Exit liquid flow distribution in Prewetted beds

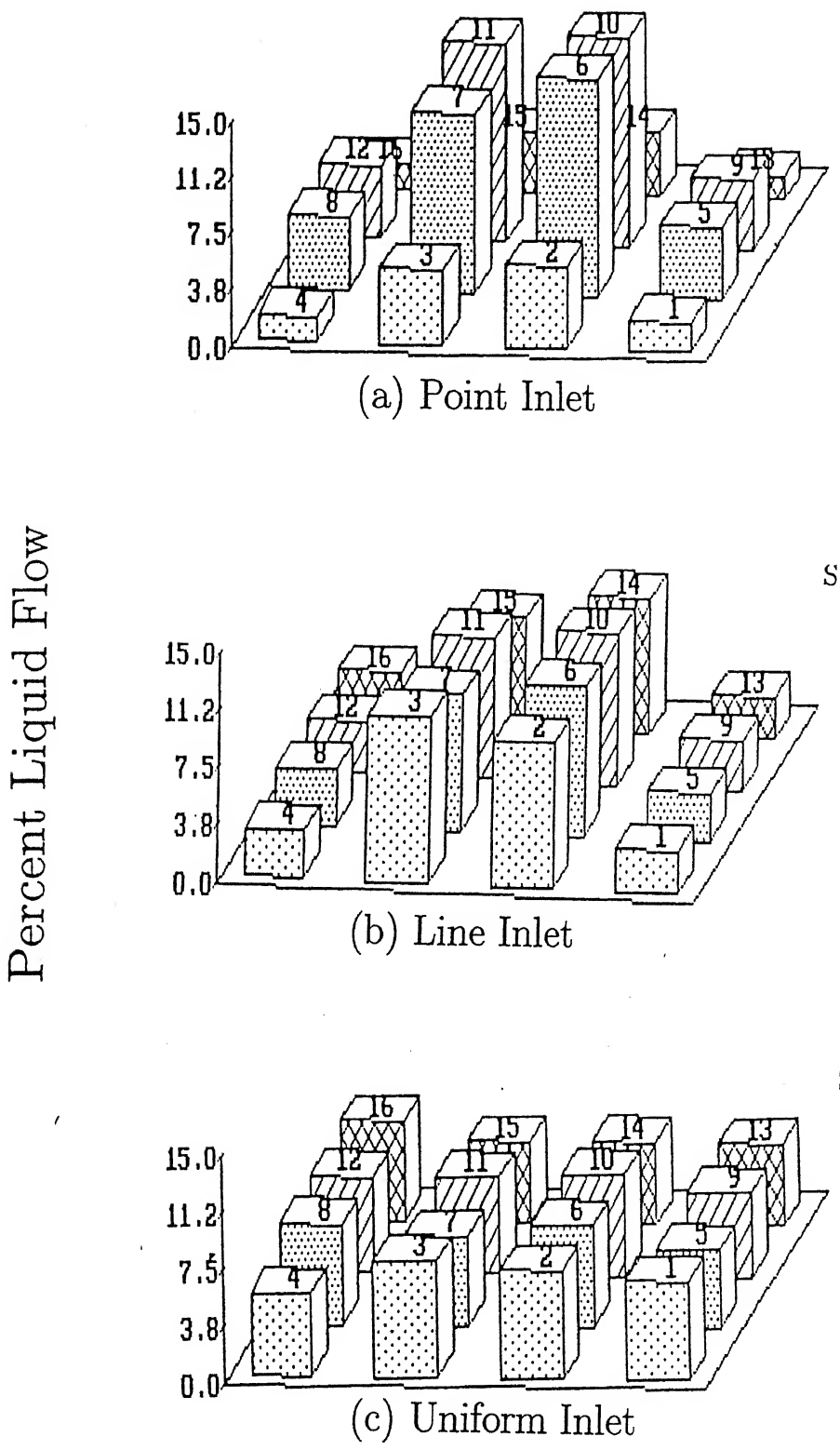

Fig. 4.8 Exit liquid flow distribution in Prewetted beds

can be observed that all the cells receive liquid though the cells in the middle receive much of it. Figure 4.3(b) is a typical experimentally observed exit flow distribution for prewetted bed with line inlet. Comparison results obtained through simulations with those of experimental ones goes in the same lines as with prewetted bed with point inlet.

Uniform inlet:

Figure 4.7(c) and 4.8(c) show exit liquid distributions simulated for prewetted bed with dimensions 40 × 40 × 45.23 mm and 40 × 40 × 94.63 mm respectively. This can be compared with similar experimental situation of prewetted bed with uniform inlet (Fig. 4.4(b)). All the cells receive liquid more or less uniformly.

4.3.1.3 A Comparison :

A comparison between the theoretically obtained exit distribution and that of the experimental one is made by using 3.5 mm diameter particles. A bed of 70 × 70 mm with a height of 201.71 mm is generated and exit flow distribution with uniform inlet is simulated for both nonprewetted and prewetted cases. This is compared with exit distributions obtained for a bed of 60 mm × 80 mm and height 200 mm under similar conditions. Figure 4.9 shows exit distributions with uniform inlet in nonprewetted and prewetted beds for both experimental and theoretical cases. Standard deviations obtained for nonprewetted bed are 4.081 and 3.6794 for experimental and theoretical cases respectively. With prewetted bed, standard deviations for the two cases are 1.900 and 0.6506 respectively. In both the cases the standard deviation obtained through simulations are close to those obtained experimentally. Difference in cross sections of the beds may be one reason for variation in standard deviations of theoretical and experimental cases. With nonprewetted bed, maldistribution can be implied from variation in percent flow rates through individual cells and channelling from inactive cells. With the prewetted bed, the exit distribution obtained was more uniform compared to that of experimental one. However, it may be

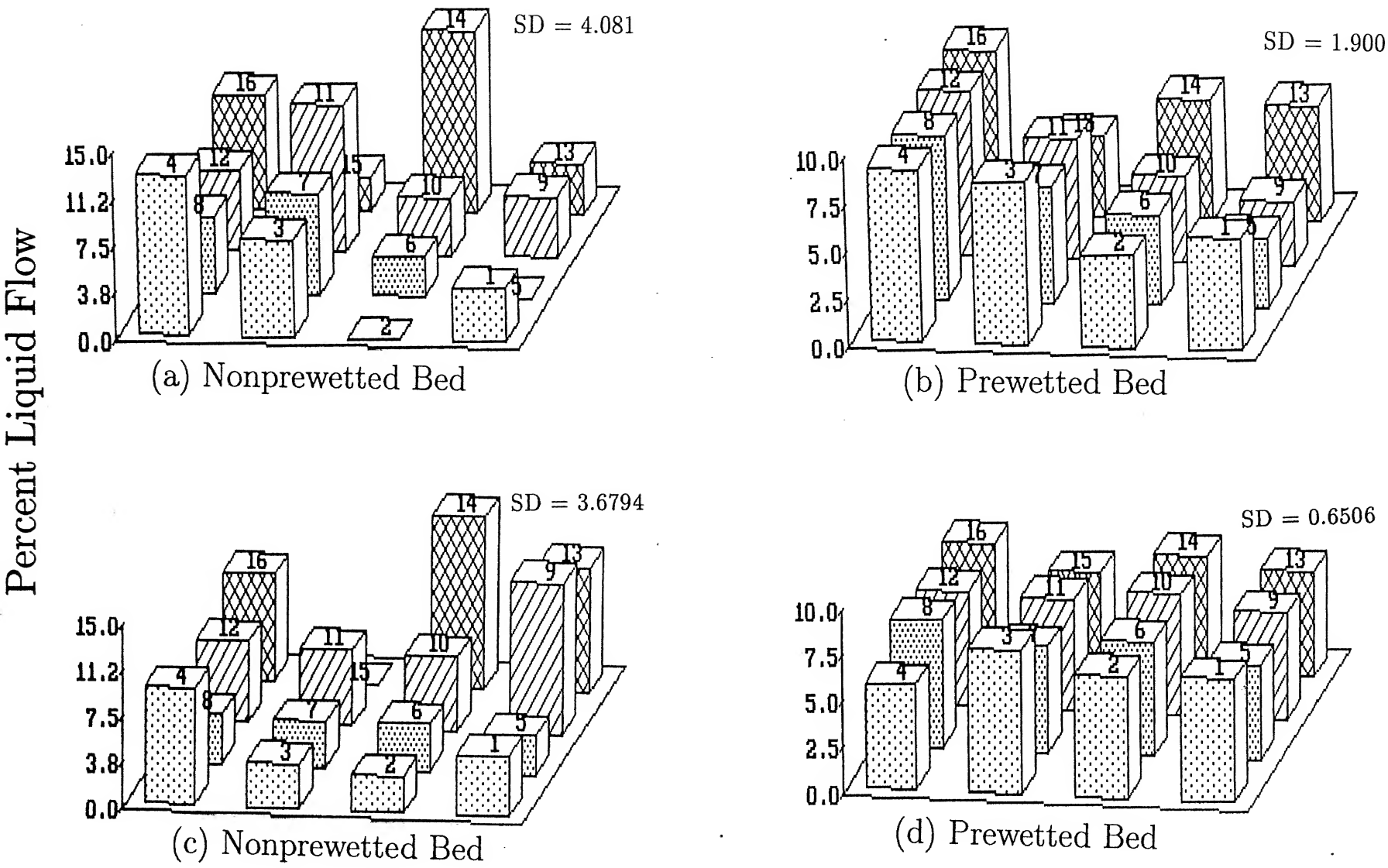

Fig. 4.9 Exit liquid flow distribution with Uniform Inlet distributor
$d_p = 3.5\,mm$, $L = 1\ kg/m^2.s$
a,b : Bed size : $60 \times 80 \times 200\,mm$ (Adapted from Ravindra., 1995)
c,d : Bed size : $70 \times 70 \times 200\,mm$ (Simulation)

because the model does not take into account liquid bridges and pockets which make a considerable proportion in prewetted bed.

4.3.1.4 Summary

A bed of dimensions 40 × 40 mm with height 45.23 mm is simulated with 9000 spheres of 2.0 mm diameter. Different inlet configurations such as point inlet, line inlet and uniform inlet has been imposed and flow distributions have been simulated for the cases of nonprewetted bed and prewetted beds. The simulation results are compared with the distribution profiles observed by Ravindra (1995). It can be seen that the channelling in the case of nonprewetted bed point inlet; maldistribution of liquid in different cells in the case of line and uniform inlets of nonprewetted bed; uniform distribution of liquid with prewetted bed uniform inlet can be clearly depicted.

4.3.2 Liquid flow rate

Liquid flow rate has pronounced effect on the way the liquid distributes in a trickle-bed reactor. Ravindra (1995) studied the variation of liquid flow texture by taking photographs (not shown here) of nonprewetted bed with uniform inlet and has observed that the maldistribution present at low flow rates decreases as the input flow rate increases and liquid spreads to all the cross sections. However, for the case of prewetted beds, not much variation with the flow rate was observed.

In this part of the study a sample bed of 50 × 50 mm with height 93.69 mm is generated with 9000 particles of radius 3.0 mm to study the effect of liquid flow rate. Liquid flow distribution has been simulated for point, line and uniform inlet configurations with nonprewetted and prewetted bed conditions. Results obtained are briefly discussed.

4.3.2.1 Point Inlet

Nonprewetted bed:

Figures 4.10(a), 4.10(b) and 4.10(c) show the exit distribution of liquid for the flow rates of 1 $kg/m^2.s$, 3 $kg/m^2.s$ and 5 $kg/m^2.s$ respectively. The standard deviation which is 10.163 in the case of 1 $kg/m^2.s$ flow rate decreased to 8.2135 for 3 $kg/m^2.s$ and further reduced to 6.2167 for 5 $kg/m^2.s$.

By comparing the exit liquid distribution in different cells of these cases, one can notice that there is spread of liquid as the flow rate increased. It can also be noticed that the cell which received more liquid when the flow rate is 1 $kg/m^2.s$ received smaller amount in the 3 $kg/m^2.s$ case and still lower amount in the 5 $kg/m^2.s$ case. Moreover, there is decrease in no. of cells those are inactive as the flow rate is increasing.

Prewetted bed :

Figure 4.11 shows the exit liquid distributions from prewetted bed with point inlet. This can be compared with Figure 4.10(c) which is for a flow rate of 5 $kg/m^2.s$. It can be seen that there are few cells in the Figure 4.10(c) (for 5 $kg/m^2.s$) where there is no flow of liquid. However, Figure 4.11 (prewetted bed case) shows that all the cells are active. The standard deviation in the former case is 6.2167 which has been decreased to 5.2895 in the case of prewetted bed. Thus it may be expected that as the flow rate increases the liquid flow distribution behaviour will approach that of prewetted bed.

4.3.2.2 Line inlet

Nonprewetted bed :

The behaviour of the bed is similar to point inlet. Figures 4.12(a), 4.12(b) and 4.12(c) show the exit flow distribution for 1 $kg/m^2.s$, 3 $kg/m^2.s$ and 5 $kg/m^2.s$ of the bed with line inlet. The standard deviations in these cases are 8.7704, 5.932 and 5.002 respectively.

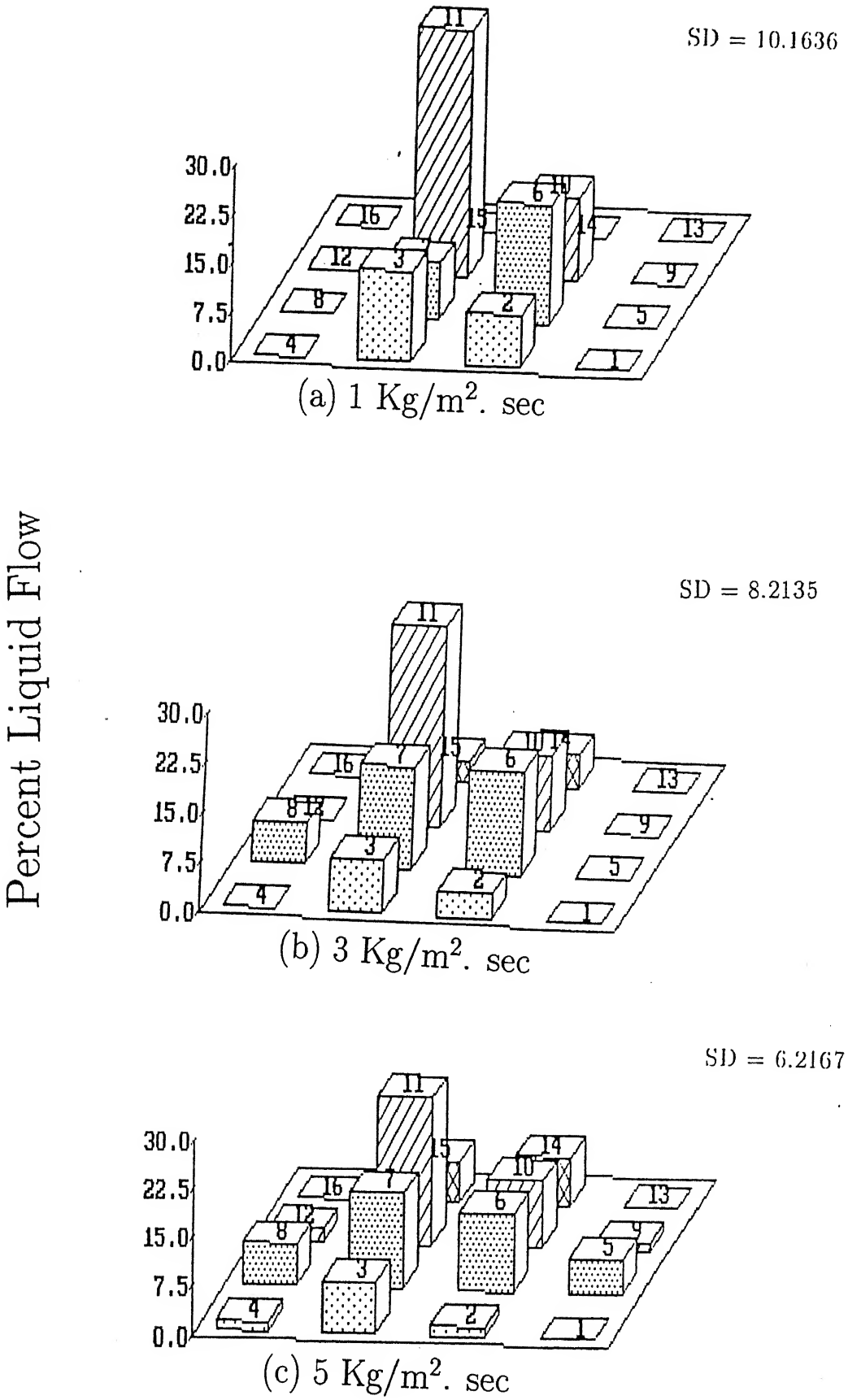

Fig. 4.10 Exit liquid flow distribution in Nonprewetted beds

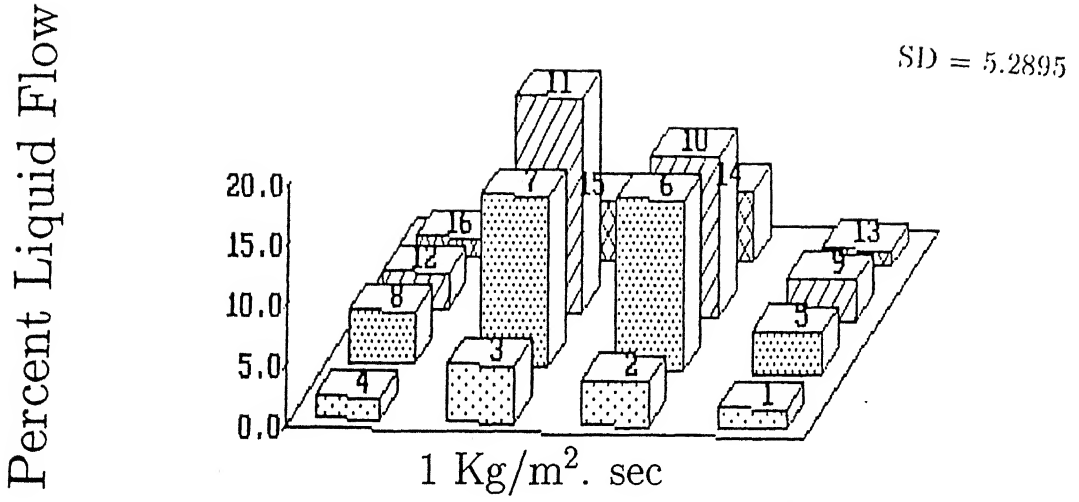

Fig. 4.11 Exit liquid flow distribution in Prewetted beds
Point Inlet, $d_p = 3.0$ mm, L = 1 kg/m^2.s, Bed size : 50 × 50 × 93.69 mm

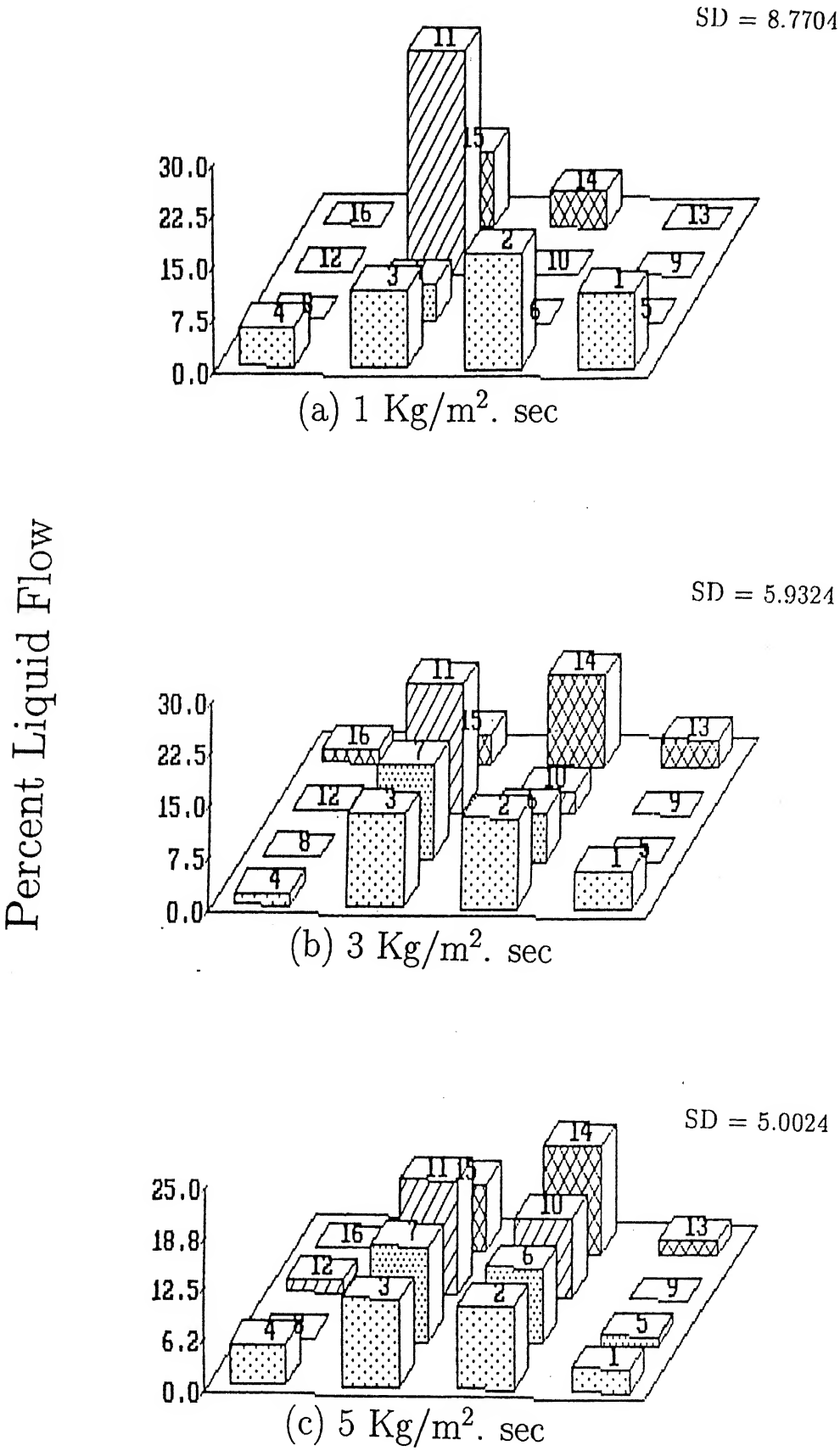

Fig. 4.12 Exit liquid flow distribution in Nonprewetted beds
Line Inlet, d_p = 3.0 mm, Bed size : 50 × 50 × 93.69 mm
a : 1 Kg/m².s b : 3 Kg/m².s c : 5 Kg/m².s

comparison of the three Figures shows that the maldistribution which was severe in the case of 1 $kg/m^2.s$ has gradually decreased. The cells which were inactive initially became active as the flow rate is increased.

Prewetted bed :

The exit flow distribution of prewetted bed is shown in the Figure 4.13. All the cells does receive the liquid though majority of flow occurs through the middle rows. The standard deviations of 5 $kg/m^2.s$ case and prewetted case are 5.002 and 3.7852 respectively.

4.3.2.3 Uniform inlet

Nonprewetted bed :

Figures 4.14(a), 4.14(b) and 4.14(c) show the exit distributions from the bed with uniform inlet for 1 $kg/m^2.s$, 3 $kg/m^2.s$ and 5 $kg/m^2.s$ respectively. The standard deviations are 5.614, 4.3585 and 2.8335 respectively. It can be noticed from the Figures that in the case of 1 $kg/m^2.s$ (Fig. 4.14(a)), cell no. 8 does not receive any liquid while cells numbered 9, 10, 13 and 14 received a flow rate less than 1.5%. With 3 $kg/m^2.s$ (Fig. 4.14(b)), all the cells does receive liquid but the cells 9 and 10 received a flow rate less than 1.5% and as the flow rate increases to 5 $kg/m^2.s$ (Fig. 4.14(c)), the distribution is becomes more uniform.

Prewetted bed :

The standard deviation of the bed is 1.0025 which means that the distribution is very uniform in the case of prewetted bed with uniform inlet (Fig. 4.15). Though the results of simulation with 5 $kg/m^2.s$ (Fig. 4.14(c)) show that none of the cells is inactive, it can be seen that the distribution is more uniform with prewetted bed. However, as the liquid flow rate increases, the flow distribution may resemble that of prewetted bed.

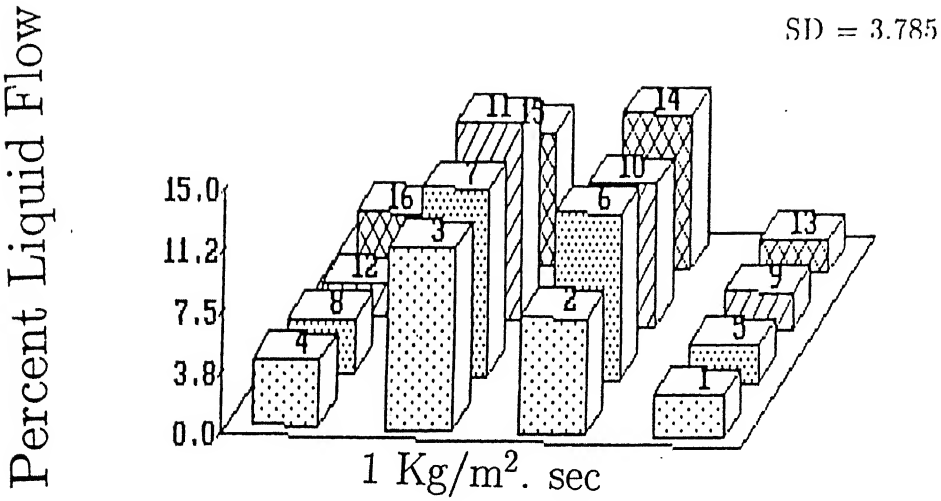

Fig. 4.13 Exit liquid flow distribution in Prewetted bed
Line Inlet, d_p = 3.0 mm, L = 1 kg/m^2.s, Bed size : 50 × 50 × 93.69 mm

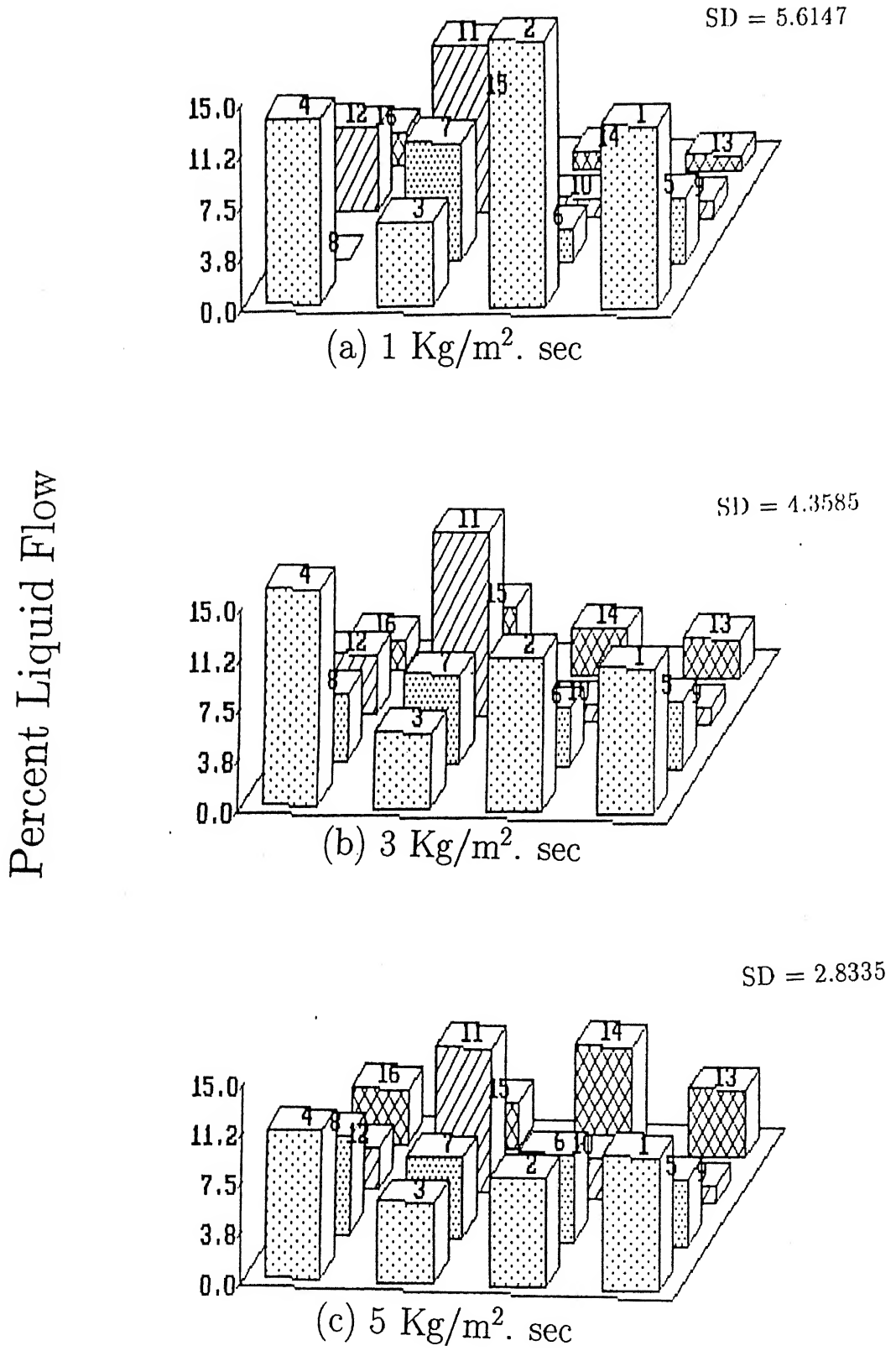

Fig. 4.14 Exit liquid flow distribution in Nonprewetted beds
Uniform Inlet, $d_p = 3.0$ mm, Bed size : 50 × 50 × 93.69 mm
a : 1 Kg/m².s b : 3 Kg/m².s c : 5 Kg/m².s

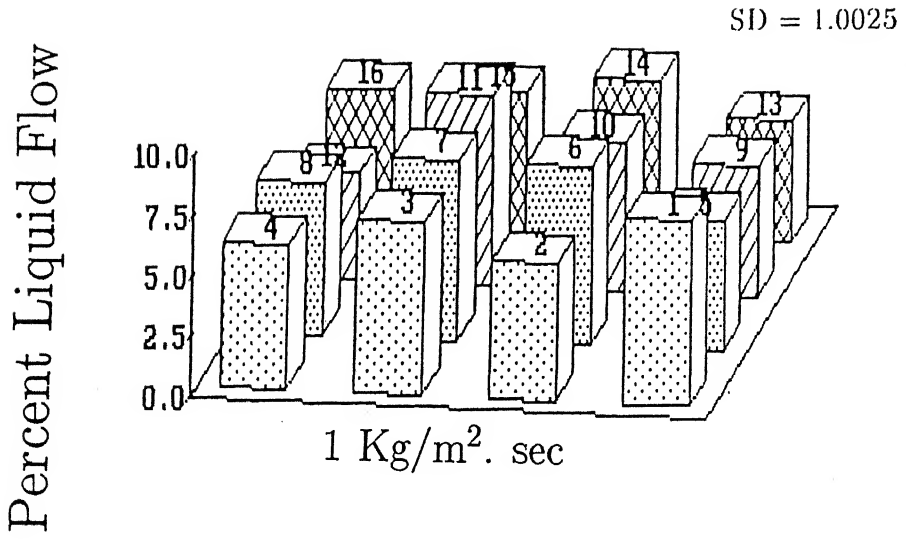

Fig. 4.15 Exit liquid flow distribution in Prewetted bed
Uniform Inlet, $d_p = 3.0\,mm$, $L = 1\ kg/m^2.s$, Bed size : $50 \times 50 \times 93.69\,mm$

4.3.3 Effect of Particle diameter

In order to study the effect of diameter of particle on the liquid flow distribution, three sets of data has been simulated. Three dimensional beds of 70 mm × 70 mm with height close to 100.0 mm are generated for particle sizes of 3.5 mm, 4.5 mm and 5.0 mm. The exit distributions are discussed for different inlet configurations.

4.3.3.1 Point inlet

A point inlet is placed at (35.0,35.0) on xy-plane for the three beds of 3.5 mm, 4.5 mm and 5.0 mm particle sizes and the distribution at the exit in these cases are shown in Figures 4.16(a), 4.16(b) and 4.16(c) respectively. Standard deviation in the case of 3.5 mm particle bed is 10.6811 and it decreased to 10.193 for 4.5 mm particle bed and further decreased to 7.25025 in the case of 5.0 mm particle diameter bed. By looking at the distribution through individual cell, it can be observed that in the case of 3.5 mm diameter bed middle cells are active and the cell no. 2 received some amount of flow rate. In the case of 4.5 mm diameter bed cells numbered 9 and 14 which were inactive in the case of 3.5 mm bed received considerable amount of liquid. But then, the cell no. 7 which was active with 3.5 mm bed did not receive any liquid with 4.5 mm bed. Also, there is variation in the percentage of liquid received by the middle cells for these two cases. In the case of 5.0 mm diameter bed also the argument goes in a similar manner. It may be ascertained from this, that, as the particle diameter varies, liquid takes different paths and thus the distribution varies.

4.3.3.2 Line inlet

The exit distribution with line inlet for different diameters of particles is shown in Figures 4.17(a), 4.17(b) and 4.17(c). Figure 4.17(a) gives the exit distribution with a bed consisting of particles of diameter 3.5 mm. Figures 4.17(b) and 4.17(c) give the exit dis-

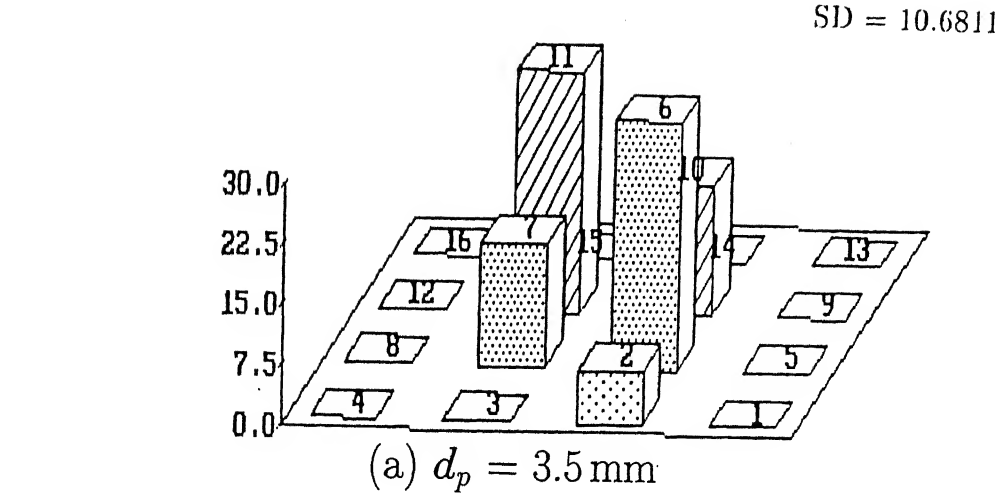

(a) $d_p = 3.5\,\text{mm}$

Percent Liquid Flow

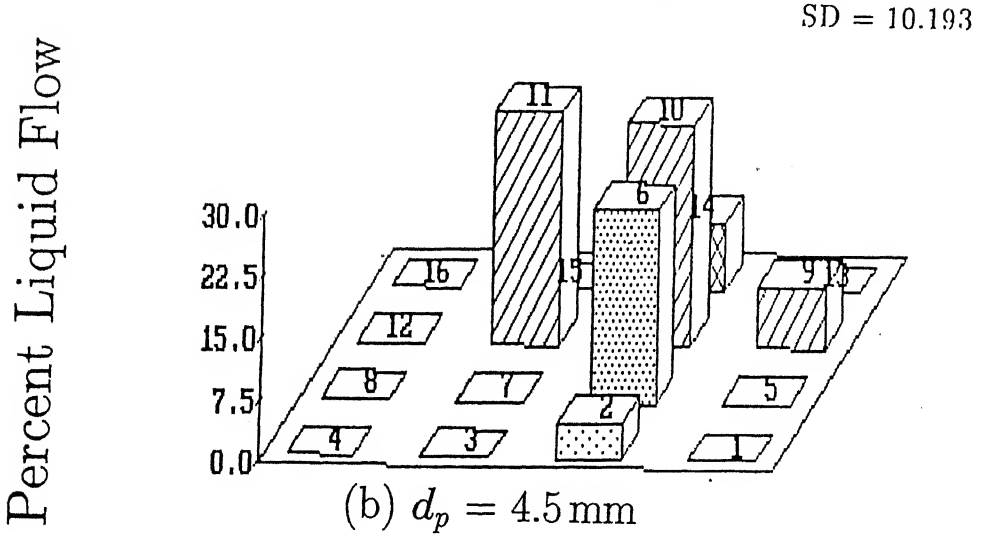

(b) $d_p = 4.5\,\text{mm}$

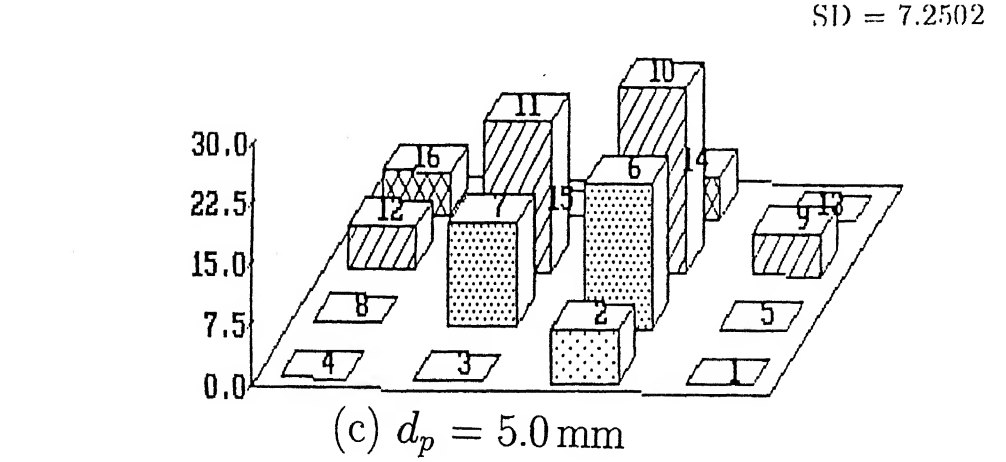

(c) $d_p = 5.0\,\text{mm}$

Fig. 4.16 Exit liquid flow distribution in Nonprewetted beds
Point Inlet, L = 1 kg/m^2.s, Bed size : 70 × 70 × 100 mm

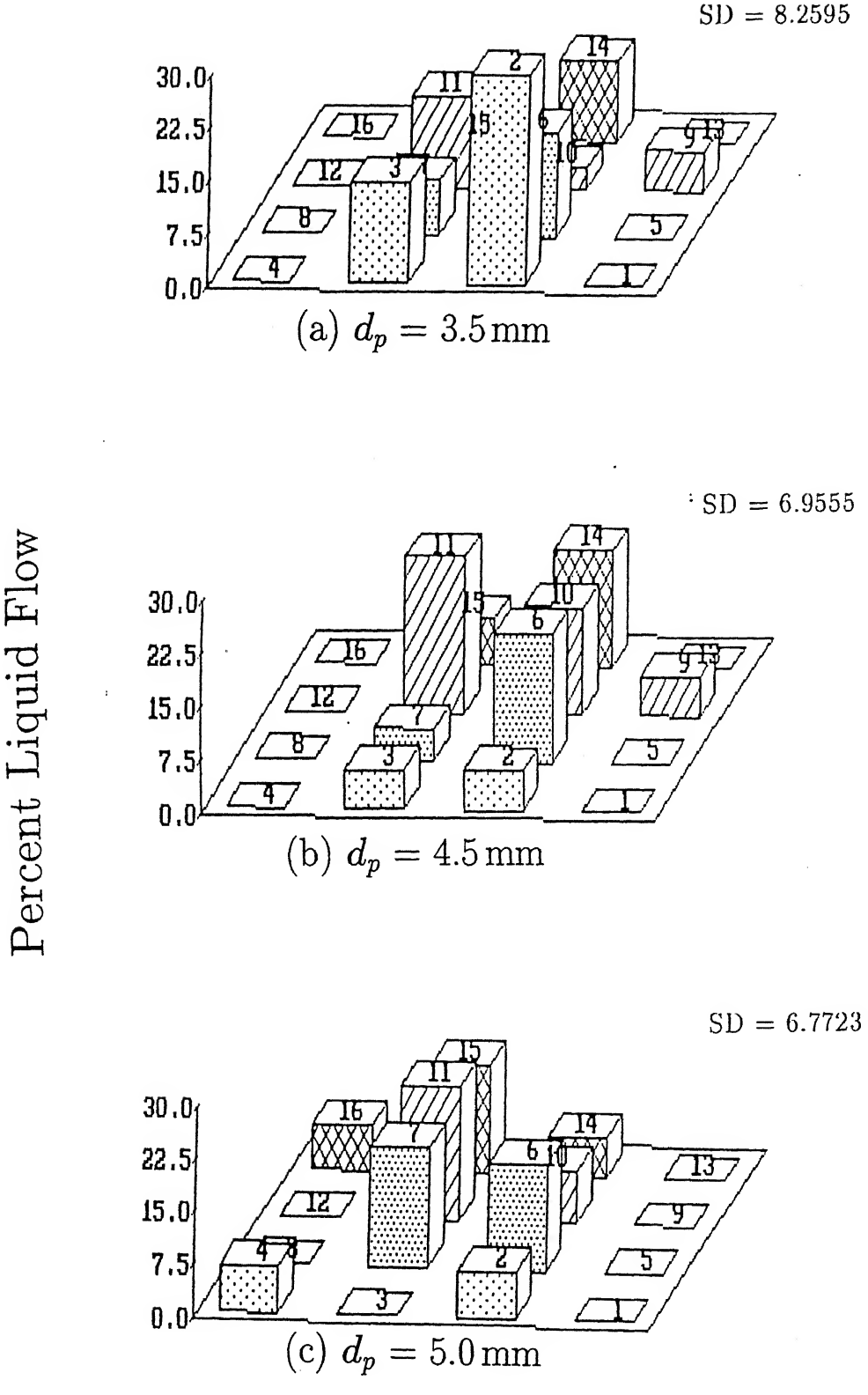

Fig. 4.17 Exit liquid flow distribution in Nonprewetted beds
Line Inlet, L = 1 kg/m^2.s, Bed size : 70 × 70 × 100 mm
a : d_p = 3.5 mm b : d_p = 4.5 mm c : d_p = 5.0 mm

tributions for beds with particle diameters of 4.5 mm and 5.0 mm respectively. For the bed with 3.5 mm diameter particles, except for the cell no. 15 all the cells in the middle row are active and also the cell no. 9 is active. For the bed with 4.5 mm particles all the cells in the middle row including the cell no. 9 are active. For the bed with 5.0 mm particles all the cells in the middle row except the cell no. 3 are active. Further more, the cells 4 and 16 are also active. Comparing these three Figures, formation of distinct and different channels could be ascertained from inactive cells of each case and variation in the flow rates received by respective cells . The standard deviations of exit distribution in these three cases are 8.2595, 7.337 and 6.772 for 3.5 mm, 4.5 mm and 5.0 mm respectively, which shows an increasing degree of uniformity in these three cases.

4.3.3.3 Uniform inlet

For the uniform inlet, the exit distributions are shown in Figures 4.18(a), 4.18(b) and 4.18(c) for the beds of 3.5 mm, 4.5 mm and 5.0 mm diameter particles respectively. In the case of 3.5 mm bed, except for the cells 8 and 15 all others are active. For 4.5 mm bed, cells 5 and 7 are the ones which are inactive and for 5.00 mm case, cells 5,8 and 13 are inactive. Looking at these exit distributions, one may easily recognize the maldistribution through distinct channel formation. Standard deviation of the distribution in cells is 4.9575, 4.7300 and 4.525 for 3.5 mm, 4.5 mm and 5.0 mm diameter packed beds respectively.

Figures 4.19(a), 4.19(b) and 4.19(c) show the exit distributions obtained by Ravindra (1995) with bed of dimensions 60 $\times$ 80 mm and height 200 mm, packed with 1.6 mm, 3.5 mm and 5.7 mm particles respectively. These Figures (4.19(a), (b) and (c)) support the argument of distinct channel formations with different diameter particles.

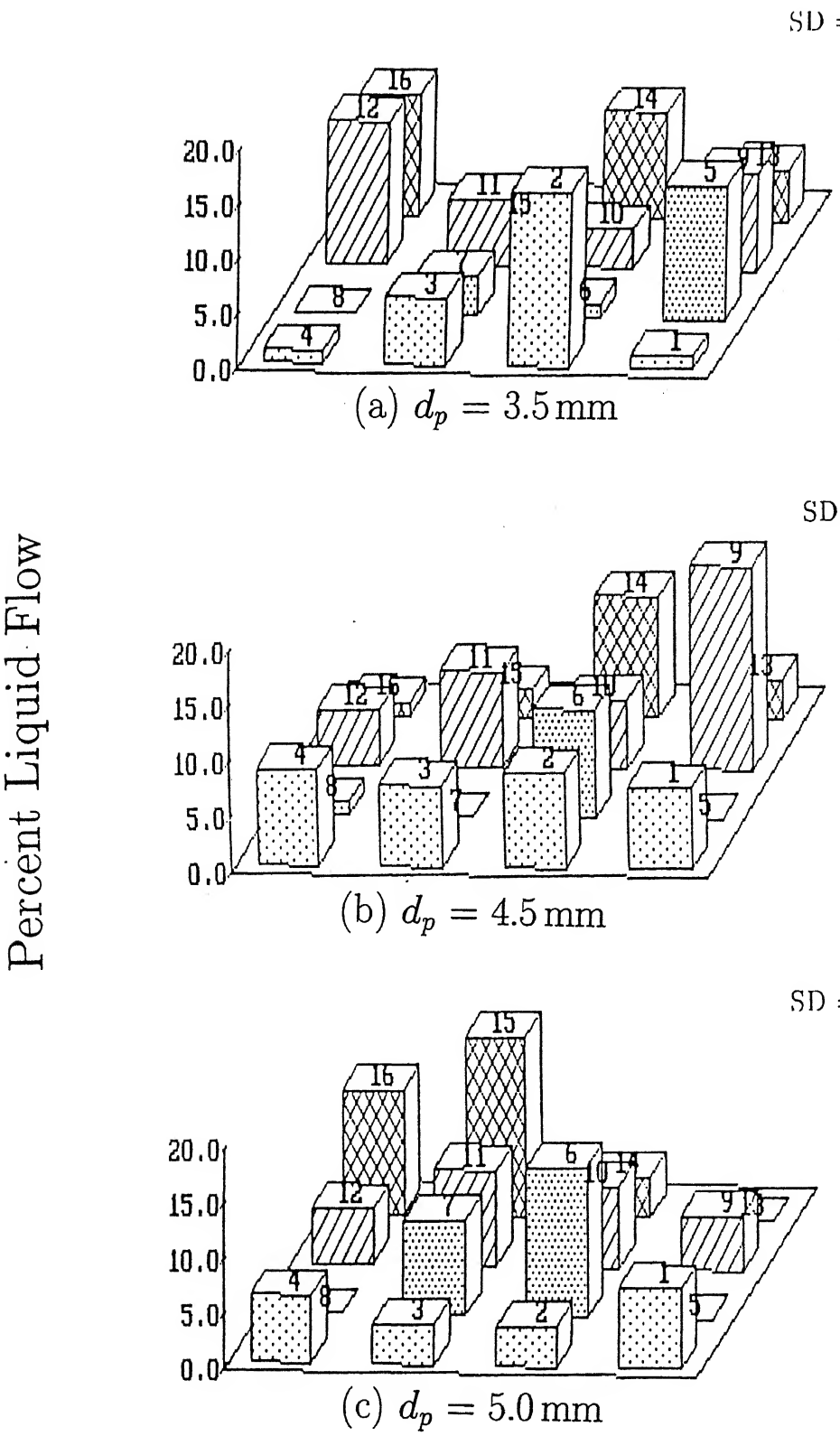

Fig. 4.18 Exit liquid flow distribution in Nonprewetted beds
Uniform Inlet, L = 1 kg/m^2.s, Bed size : 70 × 70 × 100 mm
a : d_p = 3.5 mm b : d_p = 4.5 mm c : d_p = 5.0 mm

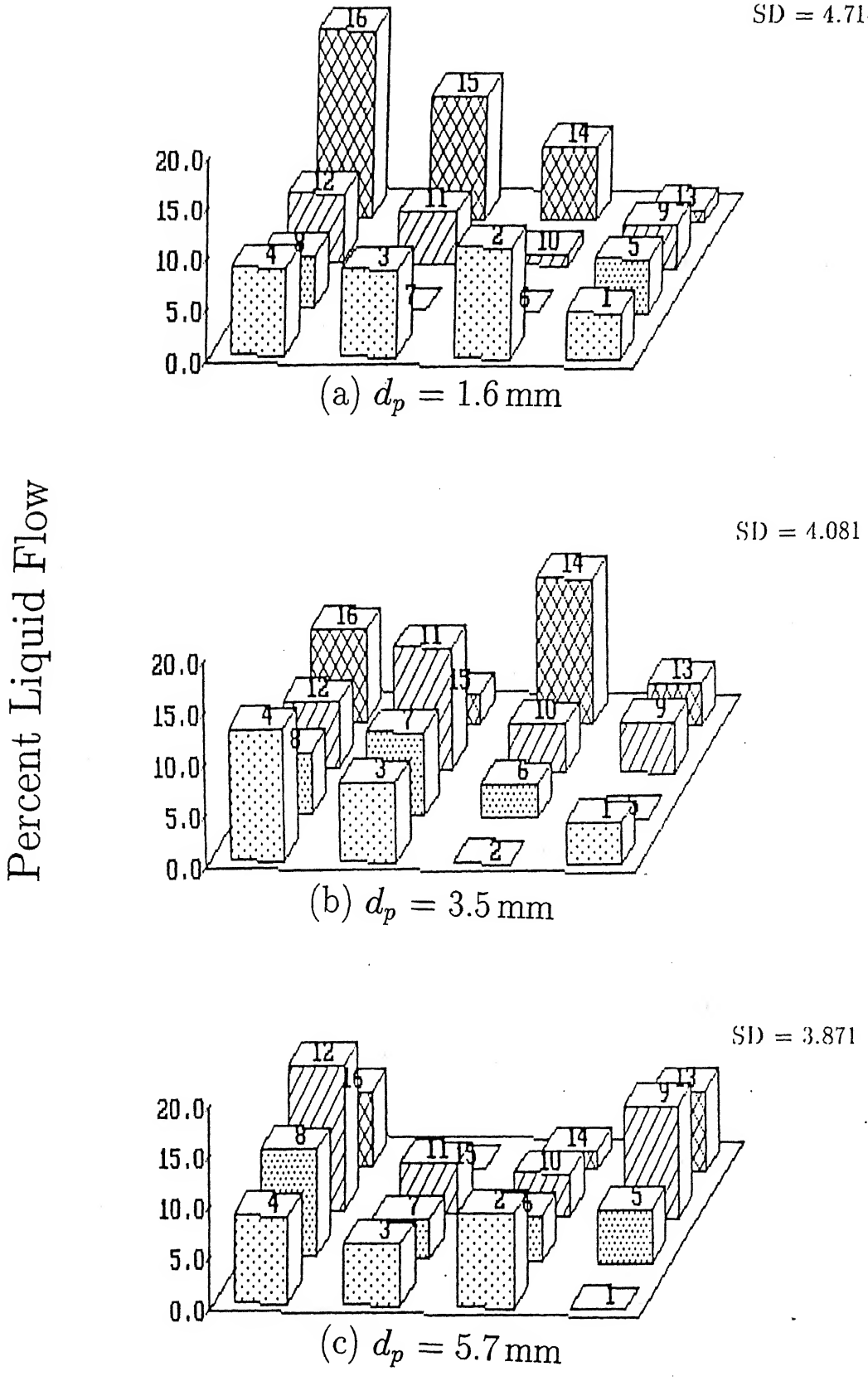

Fig. 4.19 Exit liquid flow distribution in Nonprewetted beds
Uniform Inlet, L = 1 kg/m^2.s, Bed size : 60 × 80 × 200 mm

4.3.4 Summary

A bed of 40 × 40 × 45.23 mm with 2.0 mm particles has been generated and flow distribution is studied for different inlet configurations employing both nonprewetted and prewetted beds. For nonprewetted bed, point inlet, exit distribution showed that the cells in the middle are active. This refers to the channel formation which was observed experimentally. For line and uniform inlets maldistribution of the liquid can be accounted from the cells which are empty.

In the case of prewetted bed, complete wetting which was observed experimentally can be attributed from the exit distributions which show that all the cells are active.

A bed of 50 × 50 × 93.69 mm has been generated and flow distribution has been studied for different inlet flow rates. Point, line and uniform configurations are employed and flow distribution have been studied for both nonprewetted and prewetted cases. Flow maldistribution which was severe at low flow rates, decreased considerably as the flow rate is increased.

For prewetted beds, it was experimentally found that the flow rate has very little effect on the liquid distribution. However, simulated results show no change in the standard deviation as the model does not take into account the effect of flow rate for prewetted bed.

A bed of 70 × 70 × 100 mm has been generated for particle sizes of 3.5 mm, 4.5 mm and 5.0 mm. Flow is simulated for these cases with different inputs. It is observed that the standard deviation decreases as the diameter of the particle is increases. However, maldistribution is there in each of these cases. Also an important observation is formation of distinct channels with beds of different particle sizes. These observations are vindicated by the recent experimental study by Ravindra (1995).

Exit distributions from different diameter beds revealed formation of channels at different positions. This conclusion can be supported from the argument that the formation of channels is greatly influenced by the size of particles under identical conditions.

5.2 Recommendations for future work

Present study is limited in scope because it does not incorporate liquid pockets and liquid bridges. Also the model has to be extended to incorporate gas flow. Further, validity of this model has to be checked by incorporating reaction and checking the results with experimental data obtained under identical conditions.

REFERENCES

Adams,D.J., and A. J. Matheson, "Computation of Dense Random Packing of Hard Spheres," *J. Chem. Phys.*, **56**, 1989 (1972).

Ahtchi-Ali, B., and H. Pedersen, "Very Large Lattice Model of Liquid Mixing in Trickle Beds," *Ind. Eng. Chem. Fund.*, **25**, 108 (1986).

Bemer, G.G., and F.J. Zuiderweg, "Radial Liquid Spread and Maldistribution in Packed Columns under Different Wetting Conditions," *Chem. Eng. Sci.*, **33**, 1637 (1978).

Bennett, C. H., "Seriallly Deposited Amorphous Aggregates of Hard Spheres," *J. Appl. Phys.*, **43**, 2728 (1972).

Capra, V., S. Sicardi, A. Gianetto, and J.M. Smith, "Effect of Liquid Wetting on Catalyst Effectiveness in Trickle-Bed Reactors," *Can. J. Chem. Eng.*, **60**, 282 (1982).

Christensen, G., S.J. McGovern, and S. Sundaresan, "Cocurrent Downflow of Air and Water in a Two-Dimensional Packed Column," *AIChE J.*, **32**, 1677 (1986).

Cihla, Z., and O. Schmidt, "A Study of the Flow of Liquid when Freely Trickling Over the Packing in a Cylindrical Tower," *Coll. Czech. Chem. Comm.*, **22**, 896 (1957).

Crine, M., P. Marchot, and G.A. L'Homme, "Mathematical Modeling of the Liquid Trickling Flow through a Packed Bed Using the Percolation Theory," *Comput. Chem. Eng.*, **3**, 515 (1979).

Crine, M., P. Marchot, and G.A. L'Homme, "Liquid Flow Maldistributions in Trickle-Bed Reactors," *Chem. Eng. Commun.*, **7**, 377 (1980).

Dudukovic, M.P., and P.L. Mills, "Contacting and Hydrodynamics in Trickle-Bed Reactors," *Encyclopedia of Fluid Mechanics,* N.P. Cheremisinoff, ed., Gulf Publ., Houston, Ch. 32, 969 (1986).

Funk, G.A., M.P. Harold, and K.M. Ng, "A Novel Model for Reaction in Trickle Beds with Flow Maldistribution," *Ind. Eng. Chem. Res.*, **29**, 738 (1990).

Germain, A., A.G. Lefebvre, and G.A. L'Homme, "Catalytic Trickle-Bed Reactor," *Adv. Chem. Ser.*, **No. 133**, 164 (1974).

Gianetto, A., G. Baldi, V. Specchia, and S. Sicardi, "Hydrodynamics and Solid-Liquid Contacting Effectiveness in Trickle-Bed Reactors," *AIChE J.*, **24**, 1087 (1978).

Gianetto, A., and P.L. Silveston, "*Multiphase Chemical Reactors -Theory, Design and Scale-Up*," Hemisphere Publ. Corp., Washington, (1986).

Gianetto, A., and V. Specchia, "Trickle-Bed Reactors: State of Art and Perspectives," *Chem. Eng. Sci.*, **47**, 3197 (1992).

Harold, M.P., "Impact of Wetting on Catalyst Performance in Multiphase Reaction Systems," In *Computer Aided Design of Catalysts*, Becker, E.R., and C.J. Pereira, Eds., Marcel Dekker, New York (1993).

Hartley, D. E., and W. Murgatroyd, "Criteria for the Break-Up of thin layers flowing Isothermally Over a Solid Surface," *Int. J. Heat Mass Transfer*, **7**, 1003 (1964).

Haure, P.M., R.R. Hudgins, and P.L. Silveston, "Investigation of SO_2 Oxidation Rates in Trickle-Bed Reactors Operating at Low Liquid Flow Rates," *Can. J. Chem. Eng.*, **70**, 600 (1992).

Henry, H.C., and J.B. Gilbert, "Scale-up of Pilot Plant Data for Catalytic Hydroprocessing," *Ind. Eng. Chem. Proc. Des. Dev.*, **12**, 328 (1973).

Herskowitz, M., and J.M. Smith, "Liquid Distribution in Trickle-Bed Reactors. Part-I. Flow Measurements," *AIChE J.*, **24**, 439 (1978).

Herskowitz, M., R.G. Carbonell, and J.M. Smith, "Effectiveness Factors and Mass Transfer in Trickle-Bed Reactors," *AIChE J.*, **25**, 272 (1979).

Herskowitz, M., and J.M. Smith, "Trickle-Bed Reactors: A Review," *AIChE J.*, **29**, 1 (1983).

Hofmann, H., "Hydrodynamics, Transport Phenomena, and Mathematical Models in Trickle-Bed Reactors," *Int. Chem. Eng.*, **17**, 19 (1977).

Jaffe, S.B., "Hot Spot Simulation in Commercial Hydrogenation Processes," *Ind. Eng. Chem. Proc. Des. Dev.*, **15**, 410 (1976).

Jordey, W.S., E.M. Tory, "Simulation of Random Packing of Spheres," *Simulation*, **32**, 1 (1979).

Kan, K., and P.F. Greenfield, "Multiple Hydrodynamic States in Cocurrent Two-Phase Downflow through Packed Beds," *Ind. Eng. Chem. Proc. Des. Dev.*, **17**, 482 (1978).

Kan, K., and P.F. Greenfield, "Pressure Drop and Holdup in Two-Phase Cocurrent Trickle Flows through Beds of Small Packings," *Ind. Eng. Chem. Proc. Des. Dev.*, **18**, 740 (1979).

Koros, R.M., "Catalyst Utilization in Mixed-Phase Fixed Bed Reactors," *ISCRE 4*, Heidelberg, 6-8 April (1976).

Lutran, P., K.M. Ng, and E.P. Delikat, "Liquid Distribution in Trickle Beds. An Experimental Study Using Computer-Assisted Tomography," *Ind. Eng. Chem. Res.*, **29**, 1270 (1991).

Marchot, P., M. Crine, and G.A. L'Homme, "Rational Description of Trickle Flow through Packed Beds. Part-I: Liquid Distribution far from the Distributor," *Chem. Eng. J.*, **48**, 49 (1992a).

Marchot, P., M. Crine, and G.A. L'Homme, "Rational Description of Trickle Flow through Packed Beds. Part-II: Radial Spreading of the Liquid," *Chem. Eng. J.*, **48**, 61 (1992b).

Mata, A.R., and J.M. Smith, "Oxidation of Sulfur Dioxide in a Trickle-Bed Reactor," *Chem. Eng. J.*, **22**, 229 (1981).

Matheson, A.J., "Computation of a Random Packing of Hard Spheres," *J. Phys. C: Solid State Phys.*, **7**, 2569 (1974).

Mears, D.E., "The Role of the Liquid Holdup and Effective Wetting on the Performance of Trickle-Bed Reactors," *ACS Monograph Ser.*, **No. 133**, 218 (1974).

Melli, T.R., J.M. de Santos, W.B. Kolb, and L.E. Scriven, "Cocurrent Downflow in Networks of Passages, Microscale Roots of Macroscale Flow Regimes," *Ind. Eng. Chem. Res.*, **29**, 2367 (1990).

Melli, T.R., and L.E. Scriven, "Theory of Two-Phase Cocurrent Downflow in Networks of Passages," *Ind. Eng. Chem. Res.*, **30**, 951 (1991).

Mills, P.L., and M.P. Dudukovic, "Evaluation of Liquid-Solid Contacting in Trickle-Bed Reactors by Tracer Methods," *AIChE J.*, **27**, 893 (1981).

Mills, P.L., and M.P. Dudukovic, "A Comparison of Current Models for Isothermal Trickle-Bed Reactors. Application to a Model Reaction System,' *Chemical and Catalytic Reactor Modeling,* M.P. Dudukovic and P.L. Mills, eds., *Am. Chem. Soc. Symp. Ser.,* **No. 237**, 37 (1984).

Monika Bargeil, *A C language program for settling of hard spheres in 3-dimensional space*, Mont-Allison University, Canada (1990).

Paraskos, J.A., J.A. Frayer, and Y.T. Shah, "Effect of Holdup, Incomplete Wetting and Backmixing during Hydroprocessing in Trickle-Bed Reactors," *Ind. Eng. Chem. Proc. Des. Dev.*, **14**, 315 (1975).

Powell, M.J., "Computer-Simulated Random Packing of Hard Spheres," *Powder Tech.*, **25**, 45 (1980).

Ramachandran, P.A., and R.V. Chaudhari, "*Three-Phase Catalytic Reactors*," Gordon and Breach, New York (1983).

Ravindra, P.V., *Ph.D Dissertation*, Indian Institute of Technology, Kanpur (1995).

Reddy, P.N., D.P. Rao, and M.S. Rao, "The Texture of Liquid Flow in Trickle-Bed Reactors," *Chem. Eng. Sci.*, **45**, 3193 (1990).

Satterfield, C.N., "Trickle-Bed Reactors," *AIChE J.*, **21**, 209 (1975).

Shah, Y.T., *Gas-Liquid-Solid Reactor Design*, McGraw-Hill, NY (1979).

Stanek, V., and V. Kolar, "Distribution of Liquid over a Random Packing, VIII," *Coll. Czech. Chem. Commun.*, **38**, 2865 (1973).

Stanek, V., J. Hanika, V. Hlavacek, and O. Trnka, "The Effect of Liquid Flow Distribution on the Behavior of a Trickle-Bed Reactor," *Chem. Eng. Sci.*, **36**, 1045 (1981).

Tory, E.M., B.H. Church, M.K. Tam, M. Ratner, "Simulated Random Packing of Equal Spheres," *Can. J. Chem. Eng.*, **51**, 484 (1973).

Tour, R.S., and F. Lerman, "Area Source Liquid Distribution through Unconfined Tower Packings," *Trans. Am. Inst. Chem. Eng.*, **40**, 79 (1944).

Tsochatzidis, N.A., and A.J. Karabelas, "Experiments in Trickle Beds at the Micro- and Macroscale. Flow Characterization and Onset of Pulsing," *Ind. Eng. Chem. Res.*, **33**, 1299 (1994).

van Klinken, J., and R.H. van Dongen, "Catalyst Dilution for Improved Performance of Laboratory Trickle Flow Reactors," *Chem. Eng. Sci.*, **35**, 59 (1980).

Visscher, W.M., N. Bolsterli., "Random Packing of Equal and Unequal Spheres in Two and Three Dimensions," *Nature*, **239**, 504 (1972).

Weekman, Jr., V.W., and J.E. Myers, "Fluid-Flow Characteristics of Cocurrent Gas-Liquid Flow in Packed Beds," *AIChE J.*, **10**, 951 (1964).

Zimmerman, S.P., and K.M. Ng, "Liquid Distribution in Trickling Flow Trickle-Bed Reactors," *Chem. Eng. Sci.*, **41**, 861 (1986).

Zimmerman, S.P., C.F. Chu, and K.M. Ng, "Axial and Radial Dispersion in Trickle-Bed Reactors with Trickling Gas-Liquid Down-Flow," *Chem. Eng. Commun.*, **50**, 213 (1987).